

# Graphical lasso for extremes

Phyllis Wan\*

Chen Zhou†

## Abstract

In this paper, we estimate the sparse dependence structure in the tail region of a multivariate random vector, potentially of high dimension. The tail dependence is modeled via a graphical model for extremes embedded in the Hüsler-Reiss distribution. We propose the *extreme graphical lasso* procedure to estimate the sparsity in the tail dependence, similar to the Gaussian graphical lasso in high dimensional statistics. We prove its consistency in identifying the graph structure and estimating model parameters. The efficiency and accuracy of the proposed method are illustrated by simulations and real data examples.

*Keywords and phrases:* graphical lasso; graphical models; multivariate extreme value statistics; high dimensional statistics; Hüsler-Reiss distribution.

*AMS 2010 Classification:* 62G32; 62H12; 62F12.

## 1 Introduction

Consider a Gaussian random vector with mean zero and covariance matrix  $\Sigma$ . In a Gaussian graphical model, the precision matrix  $\Theta := \Sigma^{-1}$  encodes the conditional dependence structure among the variables – variables  $i$  and  $j$  are conditionally independent given the rest of the variables if and only if  $\Theta_{ij} = 0$ , see, e.g. Lauritzen (1996).

Given an estimate of the covariance matrix  $\hat{\Sigma}$ , the *graphical lasso* method estimates a sparse  $\Theta$  using  $L_1$ -regularization by

$$\arg \min_{\Theta} \left\{ -\log |\Theta| + \text{tr} \left( \hat{\Sigma} \Theta \right) + \gamma \sum_{i \neq j} |\Theta_{ij}| \right\}, \quad (1.1)$$

where  $\gamma$  is a tuning parameter for regularization; see, e.g. Yuan and Lin (2007), Banerjee et al. (2008) and Friedman et al. (2008). The advantage of the graphical lasso method is two folds. First, it reveals the conditional dependence among the underlying random variables by producing a sparse estimate of  $\Theta$ . Second, it provides a reliable estimation of  $\Theta$  and  $\Sigma$  in the high dimensional

---

\*Erasmus University Rotterdam; Econometric Institute, Burg. Oudlaan 50, 3062 PA Rotterdam, the Netherlands; email: wan@ese.eur.nl

†Erasmus University Rotterdam; Econometric Institute, Burg. Oudlaan 50, 3062 PA Rotterdam, the Netherlands; email: zhou@ese.eur.nl

case where classical covariance estimation fails. The theoretical properties of the graphical lasso procedure are investigated in Rothman et al. (2008) and Ravikumar et al. (2011).

In this paper, we aim to estimate the sparse dependence structure in the *tail region* among high dimensional random variables. With the characterization of tail dependence, one can further conduct statistical risk assessment of extreme (co-)occurrences, such as systemic banking failures (e.g. Zhou, 2010) or compound environmental events (e.g. Coles and Tawn, 1991). Our approach is built on the framework of Engelke and Hitz (2020), which introduces graphical models for extremes by defining the conditional dependence in the tail distribution.

A parametric distribution family that can accommodate sparse graphical models for extremes is the Hüsler-Reiss (HR) distribution (Hüsler and Reiss, 1989). The class of HR distributions describes the non-trivial limiting tail distributions of Gaussian triangular arrays. Similar to Gaussian distribution, it is parametrized by bilateral relations. More specifically, a  $d$ -dimensional HR graphical model can be parametrized by a precision matrix  $\Theta \in \mathbb{R}^{d \times d}$ , such that the variables  $i$  and  $j$  are conditionally independent in the extremes given the rest of the variables if and only if  $\Theta_{ij} = 0$  (Engelke and Hitz, 2020, Hentschel et al., 2022).

Unlike the Gaussian case, the precision matrix  $\Theta$  in the HR model is not of full rank. Due to this low-rank property, existing statistical inference procedures for estimating  $\Theta$  in an HR model often start with conditioning on a chosen dimension being above a high threshold. In turn, one can only estimate  $\Theta^{(k)} \in \mathbb{R}^{(d-1) \times (d-1)}$ , the submatrix of  $\Theta$  where the  $k$ -th row and  $k$ -th column are removed (Engelke and Hitz, 2020). Estimating an HR graphical model is therefore challenging when a sparse  $\Theta$  is desired: a sparse estimate of  $\Theta^{(k)}$  does not guarantee sparsity on the omitted  $k$ -th row and column. Hentschel et al. (2022) propose an estimation procedure for  $\Theta$  using matrix completion when the sparsity structure of  $\Theta$  was known. To date, the only sparse estimation for  $\Theta$  without knowing the sparsity structure ex-ante is proposed by Engelke et al. (2022). They achieve this goal by aggregating sparse estimates of  $\Theta^{(k)}$  for all  $k = 1, \dots, d$  using a majority vote to decide whether or not each entry of  $\Theta$  should be zero. In other words, their estimation procedure requires estimating  $d$  graphical models, which can be computationally intensive for large  $d$ .

In this paper, we propose a direct estimate of  $\Theta$  with a built-in option for sparse estimation via  $L_1$ -regularization. We term it the *extreme graphical lasso*. The core idea is as follows. We show that by adding a positive constant  $c$  to each entry of  $\Theta$ , the matrix

$$\Theta^* := \Theta + c\mathbf{1}\mathbf{1}^T$$

is the inverse of a covariance matrix  $\Sigma^*$  which can be estimated consistently from observations. To impose sparsity on the entries of  $\Theta$ , we only need to estimate  $\Theta^*$  by shrinking the off-diagonal entries to  $c$ , which can be achieved in the optimization

$$\arg \min_{\Theta^*} \left\{ -\log |\Theta^*| + \text{tr} \left( \hat{\Sigma}^* \Theta^* \right) + \gamma \sum_{i \neq j} |\Theta_{ij}^* - c| \right\},$$

where  $\gamma > 0$  is the regularization parameter. The extreme graphical lasso requires solving only one optimization problem and therefore is efficient in handling large dimensions. In addition, it

can achieve both graph structure identification and parameters estimation simultaneously in high dimensional settings. The efficiency and accuracy are the main advantages of this novel method.

We provide finite sample theory and asymptotic theory for the extreme graphical lasso. In particular, we show a consistent identification of the graph and accurate estimation of the non-sparse parameters in  $\Theta$ . We provide practical guidance in choosing the tuning parameters for applying the extreme graphical lasso method, based on theoretical motivations. The performance of the proposed method is shown by simulations. Finally, we apply the extreme graphical lasso to two real data examples to illustrate its usefulness in uncovering underlying dependence structure of extreme events.

The remainder of the paper is structured as follows. The background for HR graphical models and new insights regarding its parametrizations are presented in Section 2. The extreme graphical lasso method is introduced in Section 3. The finite sample and asymptotic theories are shown in Sections 4 and 5. Finally, the performance of the method is illustrated in Sections 6 and 7.

## 1.1 Notation

We adopt the following notation. Let  $\mathbf{0}$  and  $\mathbf{1}$  denote vectors whose elements are all 0's and all 1's respectively. We allow them to denote vectors of different length in different contexts when there are no possibilities of confusion. Let  $\mathbf{e}_j$  denote the vector such that

$$\mathbf{e}_j = \underbrace{(0, \dots, 0, 1, 0, \dots, 0)^T}_{\text{Only the } j\text{-th entry is 1.}}$$

Given a square matrix  $A$ ,  $A \succ 0$  and  $A \succeq 0$  denote the fact that  $A$  is positive definite and positive semi-definite, respectively. For the matrix norms:  $\|\cdot\|_\infty$  is the element-wise  $L_\infty$ -norm, both for vectors and matrices;  $|||\cdot|||_\infty$  is the  $l_\infty$ -operator norm for matrices, i.e. the row-wise maxima of  $L_1$ -norms applied to each row. We note the following properties of these norms:

- Both  $\|\cdot\|_\infty$  and  $|||\cdot|||_\infty$  are norms.
- For matrix  $A$  and vector  $v$ ,  $\|Av\|_\infty \leq |||A|||_\infty \|v\|_\infty$ .
- For matrices  $A$  and  $B$  with compatible dimensions,  $|||AB|||_\infty \leq |||A|||_\infty |||B|||_\infty$ .

## 2 Hüsler-Reiss graphical models

In this section, we describe the class of HR graphical models. In particular, we offer new insights into its various parametrizations, including their geometric interpretations and their connections to each other.

### 2.1 Graphical models for extremes

Consider a random vector  $\mathbf{X} = (X_1, \dots, X_d)$ . Denote  $\tilde{X}_k = \frac{1}{1-F_k(X_k)}$ , where  $F_k$  is the marginal distribution function of  $X_k$ . Then  $\tilde{\mathbf{X}} = (\tilde{X}_1, \dots, \tilde{X}_d)$  is a random vector with standard Pareto

marginals and summarizes the dependence structure of  $\mathbf{X}$ . Following multivariate extreme value theory, we assume that  $\tilde{\mathbf{X}}$  belongs to the domain of attraction of a multivariate extreme value distribution, i.e. the limit of its component-wise maxima converges to a non-degenerate distribution. Specifically, given i.i.d. copies of  $\tilde{\mathbf{X}}$ ,  $\tilde{\mathbf{X}}^i = (\tilde{X}_1^i, \dots, \tilde{X}_d^i), i \in \mathbb{N}$ , there exists a random vector  $\mathbf{Z} = (Z_1, \dots, Z_d)$  such that

$$P(\mathbf{Z} \leq \mathbf{z}) := \lim_{n \rightarrow \infty} P\left(\max_{i=1, \dots, n} \tilde{X}_1^i \leq nz_1, \dots, \max_{i=1, \dots, n} \tilde{X}_d^i \leq nz_d\right) = G(\mathbf{z}), \quad (2.1)$$

where each marginal distribution of  $G$  is Fréchet-distributed. By writing

$$G(\mathbf{z}) = \exp(-\Lambda(\mathbf{z})),$$

where  $\Lambda$  is a Radon measure on the cone  $\mathcal{E} = [0, \infty)^d \setminus \{\mathbf{0}\}$  and  $\Lambda(\mathbf{z})$  is shorthand for  $\Lambda([0, \infty)^d \setminus [\mathbf{0}, \mathbf{z}])$ , the measure  $\Lambda$  is known as the exponent measure and characterizes the dependence structure of  $\mathbf{X}$  in the tail region, see, e.g. de Haan and Ferreira (2006, Chapter 6.1).

The domain of attraction condition (2.1) can be equivalently expressed in terms of threshold exceeding. Consider the exceedances of  $\tilde{\mathbf{X}}$  where its  $L_\infty$ -norm  $\|\tilde{\mathbf{X}}\|_\infty$  is higher than a certain threshold. There exists a random vector  $\mathbf{Y}$  such that

$$P(\mathbf{Y} \leq \mathbf{z}) := \lim_{u \rightarrow \infty} P\left(\frac{\tilde{\mathbf{X}}}{u} \leq \mathbf{z} \mid \|\tilde{\mathbf{X}}\|_\infty > u\right) = \frac{\Lambda(\mathbf{z} \wedge \mathbf{1}) - \Lambda(\mathbf{z})}{\Lambda(\mathbf{1})}. \quad (2.2)$$

Here the random vector  $\mathbf{Y}$  is defined with support on the  $L$ -shaped set  $\mathcal{L} = \{\mathbf{x} \in \mathcal{E} : \|\mathbf{x}\|_\infty > 1\}$ . Its distribution is known as a multivariate Pareto distribution; see Rootzén and Tajvidi (2006).

The framework of graphical models for extremes (Engelke and Hitz, 2020) considers the conditional independence of the threshold exceedance limit  $\mathbf{Y}$  in (2.2). Since  $\mathbf{Y}$  is defined on the  $L$ -shaped set  $\mathcal{L} = \{\mathbf{x} \in \mathcal{E} : \|\mathbf{x}\|_\infty > 1\}$ , which is not a product space, the notion of conditional independence is instead defined on the subspace  $\mathcal{L}^k = \{\mathbf{x} \in \mathcal{L} : x_k > 1\}$  for each  $k$ . Define the random vector  $\mathbf{Y}^k \stackrel{d}{=} \mathbf{Y} | Y_k > 1$ . Then  $\mathbf{Y}$  is said to exhibit conditional independence in extremes between component  $i$  and  $j$  if and only if  $Y_i^k$  and  $Y_j^k$  are conditionally independent for all  $k$ ,

$$Y_i \perp\!\!\!\perp_e Y_j | \mathbf{Y}_{\setminus \{i,j\}} \Leftrightarrow \forall k \in \{1, \dots, d\} : Y_i^k \perp\!\!\!\perp Y_j^k | \mathbf{Y}_{\setminus \{i,j\}}^k, \quad (2.3)$$

where  $\mathbf{Y}_{\setminus \{i,j\}}$  ( $\mathbf{Y}_{\setminus \{i,j\}}^k$ ) indicates all other dimensions in  $\mathbf{Y}$  ( $\mathbf{Y}^k$ ) excluding  $\{i, j\}$ .

Let  $\mathcal{G} = (V, E)$  be a graph defined by a set of nodes  $V = \{1, \dots, d\}$  and a set of undirected edges between pairs of nodes  $E \subset V \times V$ . A graphical model for extremes based on graph  $\mathcal{G}$  has a multivariate Pareto distribution  $\mathbf{Y}$  that satisfies

$$\{i, j\} \notin E \Leftrightarrow Y_i \perp\!\!\!\perp_e Y_j | \mathbf{Y}_{\setminus \{i,j\}}.$$

In the case where the exponent measure  $\Lambda$  admits a density function  $\lambda$ , the conditional independence in extreme is equivalent to the decomposition of  $\lambda$  (Engelke and Hitz, 2020):

$$Y_i \perp\!\!\!\perp_e Y_j | \mathbf{Y}_{\setminus \{i,j\}} \Leftrightarrow \lambda(\mathbf{y}) = \frac{\lambda_{\{i\}}(\mathbf{y}_{\setminus \{i\}}) \lambda_{\{j\}}(\mathbf{y}_{\setminus \{j\}})}{\lambda_{\{i,j\}}(\mathbf{y}_{\setminus \{i,j\}})}, \quad (2.4)$$

where  $\mathbf{y}_{\setminus A}$  denotes the entries of  $\mathbf{y}$  outside of the index set  $A$ .

## 2.2 Hüsler-Reiss graphical models

The class of Hüsler-Reiss (HR) distributions is the family of distributions that describes the non-trivial tail limiting distribution of Gaussian triangular arrays (Hüsler and Reiss, 1989). It has been used as a canonical parametric family and a counterpart to Gaussian distribution in modelling extremes. There exist various parametrizations of the HR distributions, the algebraic relationships between which can be found in Röttger et al. (2023). In the following, we motivate these parametrizations from a geometric point of view, which leads to simpler proofs of existing results and additional insights. The proofs of the propositions in this section are presented in Appendix A.

### 2.2.1 Characterization using variogram matrix $\Gamma$ and sub-covariance matrices $\Sigma^{(k)}$ 's

In its original definition (Hüsler and Reiss, 1989), a  $d$ -dimensional HR model is parametrized by a matrix  $\Gamma \in \mathbb{R}^{d \times d}$ , defined on the parameter space

$$\mathcal{D} = \{\Gamma | \Gamma^T = \Gamma, \text{diag}(\Gamma) = \mathbf{0}; \mathbf{x}^T \Gamma \mathbf{x} \leq 0, \text{ for any } \mathbf{x} \neq \mathbf{0} \text{ such that } \mathbf{x}^T \mathbf{1} = 0\}.$$

In this paper, we only consider the full-rank HR model defined by the sub-parameter space

$$\mathcal{D}_0 = \{\Gamma | \Gamma^T = \Gamma, \text{diag}(\Gamma) = \mathbf{0}; \mathbf{x}^T \Gamma \mathbf{x} < 0, \text{ for any } \mathbf{x} \neq \mathbf{0} \text{ such that } \mathbf{x}^T \mathbf{1} = 0\},$$

such that the exponent measure  $\Lambda$  admits a density<sup>1</sup>.

The following proposition provides the geometric interpretation of this parameter space. Although it is a well-known result, a proof is included for completeness.

**Proposition 2.1.** *Given a multivariate random vector  $\mathbf{W} = (W_1, \dots, W_d)$ , define its variogram matrix to be  $\Gamma = (\Gamma_{ij}) \in \mathbb{R}^{d \times d}$  such that*

$$\Gamma_{ij} = E(W_i - W_j)^2.$$

*The parameter space  $\mathcal{D}_0$  is the collection of variogram matrices  $\Gamma$  for all random vectors  $\mathbf{W}$  with positive definite covariance matrices.*

Given the covariance matrix  $\Sigma$  of  $\mathbf{W}$ , its variogram matrix can be derived from

$$\begin{aligned} \Gamma_{ij} &= E[(W_i - W_j)]^2 \\ &= E(W_i - W_k) - (W_j - W_k)^2 \\ &= E(W_i - W_k)^2 + E(W_j - W_k)^2 - 2E[(W_i - W_k)(W_j - W_k)] \\ &= \Sigma_{ii} + \Sigma_{jj} - 2\Sigma_{ij}. \end{aligned} \tag{2.5}$$

However, given a variogram  $\Gamma$ , the choice of covariance matrix of the corresponding random vector  $\mathbf{W}$  needs not be unique. For example, given any univariate random variable  $A$ ,  $\mathbf{W} - A \cdot \mathbf{1}$  has the

---

<sup>1</sup>The same assumption is imposed in all previous literature on extremal graphical models, such as Engelke and Hitz (2020), Engelke et al. (2022), Hentschel et al. (2022) and Röttger et al. (2023).

same variogram as  $\mathbf{W}$ . Therefore the converse of Proposition 2.1 fails: any  $\Gamma \in \mathcal{D}_0$  can also be the variogram matrix of a  $\mathbf{W}$  whose covariance matrix  $\Sigma$  is not of full rank.

It is possible to impose additional assumptions on the structure of  $\mathbf{W}$  to obtain a one-to-one correspondence between its covariance and variogram matrices. One option is to restrict  $W_k \equiv 0$  for a given  $k$ . Assume that  $\mathbf{W}$  has full-rank covariance matrix and variogram  $\Gamma$ . Consider  $\mathbf{W}^{(k)} := \mathbf{W} - W_k \cdot \mathbf{1}$ . Then  $\mathbf{W}^{(k)}$  has variogram  $\Gamma$  and covariance matrix  $\tilde{\Sigma}^{(k)}$  with its elements defined by

$$\begin{aligned} \tilde{\Sigma}_{ij}^{(k)} &:= E[W_i^{(k)} W_j^{(k)}] \\ &= E[(W_i - W_k)(W_j - W_k)] \\ &= \frac{1}{2} (E(W_i - W_k)^2 + E(W_j - W_k)^2 - E[(W_i - W_j)^2]) \\ &= \frac{1}{2} (\Gamma_{ik} + \Gamma_{jk} - \Gamma_{ij}). \end{aligned} \tag{2.6}$$

Combining (2.5) and (2.6), there exists a one-to-one transformation between  $\Gamma$  and  $\tilde{\Sigma}^{(k)}$ . Consequently, we can use  $\tilde{\Sigma}^{(k)}$ , for any fixed  $k$ , to parametrize an HR distribution. Note that  $\tilde{\Sigma}^{(k)}$  is degenerate on the  $k$ -th row and the  $k$ -th column. Let  $\Sigma^{(k)}$  be the  $(d-1) \times (d-1)$  matrix constructed by removing the  $k$ -th row and the  $k$ -th column from  $\tilde{\Sigma}^{(k)}$ . For convenience, we index the rows and columns of  $\Sigma^{(k)}$  using the original row and column numbers from  $\tilde{\Sigma}^{(k)}$ . By definition,  $\tilde{\Sigma}^{(k)}$  is of rank  $d-1$ , therefore  $\Sigma^{(k)}$  is of full rank.

This parametrization can be used to express the density of the exponent measure  $\Lambda(\cdot)$  of the HR model (Engelke et al., 2015):

$$\lambda(\mathbf{y}) = y_k^{-2} \prod_{i \neq k} y_i^{-1} \phi_d(\mathbf{y}'_k; \Sigma^{(k)}),$$

where  $\phi_d(\cdot; \Sigma^{(k)})$  is the density of a centered  $d$ -dimensional Gaussian distribution with covariance matrix  $\Sigma^{(k)}$  and  $\mathbf{y}'_k = \{\log(y_i/y_k) + \Gamma_{ik}/2\}_{i=\{1, \dots, d\} \setminus k}$ . Note again that this formula holds for any  $k = 1, \dots, d$ .

## 2.2.2 Characterization using precision matrix $\Theta$

Denote the inverse of  $\Sigma^{(k)}$  to be  $\Theta^{(k)} := (\Sigma^{(k)})^{-1}$ . It follows from the decomposition of the exponent density (2.4) that

$$Y_i \perp\!\!\!\perp_e Y_j | \mathbf{Y}_{\setminus \{i,j\}} \Leftrightarrow \Theta_{ij}^{(k)} = 0, \quad \forall k \neq i, j.$$

In other words,  $\Theta^{(k)}$  serves as the precision matrix for the graph  $\mathcal{G}$  excluding the node  $k$ . The following result from Engelke and Hitz (2020) guarantees a precision matrix  $\Theta$  for the full graph  $\mathcal{G}$ .

**Proposition 2.2** (Lemma 1, Engelke and Hitz, 2020). *For  $k \neq k'$ , the following relationships hold*

$$\begin{aligned} \Theta_{ij}^{(k')} &= \Theta_{ij}^{(k)} \quad , \quad \text{if } i, j \neq k; \\ \Theta_{ik}^{(k')} &= - \sum_{l \neq k} \Theta_{il}^{(k)} \quad , \quad \text{if } i \neq k \text{ and } j = k; \\ \Theta_{kk}^{(k')} &= \sum_{m, l \neq k} \Theta_{ml}^{(k)} \quad , \quad \text{if } i = k \text{ and } j = k. \end{aligned}$$

Define matrix  $\Theta \in \mathbb{R}^{d \times d}$  such that for any  $k$ ,

$$\begin{aligned}\Theta_{ij} &= \Theta_{ij}^{(k)} \quad , \quad \text{if } i, j \neq k; \\ \Theta_{ik} &= - \sum_{l \neq k} \Theta_{il}^{(k)} \quad , \quad \text{if } i \neq k \text{ and } j = k; \\ \Theta_{kk} &= \sum_{m, l \neq k} \Theta_{ml}^{(k)} \quad , \quad \text{if } i = k \text{ and } j = k.\end{aligned}$$

Then  $\Theta$  satisfies

$$Y_i \perp\!\!\!\perp_e Y_j | \mathbf{Y}_{\setminus \{i, j\}} \quad \Leftrightarrow \quad \Theta_{ij}^{(k)} = 0, \quad i, j \neq k \quad \Leftrightarrow \quad \Theta_{ij} = 0.$$

Hence  $\Theta$  is referred to as the *precision matrix* for the HR graphical model (Hentschel et al., 2022).

Let  $\tilde{\Theta}^{(k)}$  be the  $(d \times d)$ -matrix obtained by augmenting  $\Theta^{(k)}$  with a  $k$ -th column and a  $k$ -th row of 0 entries. Then for any  $k$ ,  $\Theta \in \mathbb{R}^{d \times d}$  can be written as

$$\Theta = (I - \mathbf{1}\mathbf{e}_k^T) \cdot \tilde{\Theta}^{(k)} \cdot (I - \mathbf{e}_k\mathbf{1}^T),$$

where recall that  $\mathbf{e}_k$  is the vector with 1 on the  $k$ -th entry and 0 everywhere else. In particular, removing the  $k$ -th column and the  $k$ -th row from  $\Theta$  results in  $\Theta^{(k)}$ . There exists one-to-one relationship between  $\Theta$  and  $\Theta^{(k)}$ , and hence  $\Sigma^{(k)}$ , for each  $k$ . Therefore  $\Theta$  can be used to parametrize an HR distribution.

### 2.2.3 Characterization using covariance matrix $\Sigma$

In the following, we define a covariance matrix which serves as the ‘inverse’ of  $\Theta$ . Given a variogram  $\Gamma$ , we consider the corresponding random vector  $\mathbf{W}$  with the restriction  $\sum_{k=1}^d W_k \equiv 0$ .

**Proposition 2.3.** *Let  $\mathbf{W}$  be a random vector with variogram  $\Gamma \in \mathcal{D}_0$ . Then the random vector  $\mathbf{W}' := \mathbf{W} - \bar{W} \cdot \mathbf{1}$  has variogram  $\Gamma$  and covariance matrix*

$$\Sigma := -\frac{1}{2} \left( I - \frac{\mathbf{1}\mathbf{1}^T}{d} \right) \Gamma \left( I - \frac{\mathbf{1}\mathbf{1}^T}{d} \right). \quad (2.7)$$

Conversely,  $\Gamma$  can be obtained from  $\Sigma$  via (2.5). Therefore  $\Sigma$  can be used to parametrize an HR distribution.

In the following, we provide the connections between  $\Sigma$ ,  $\tilde{\Sigma}^{(k)}$  and  $\Theta$ .

**Proposition 2.4** (Relationship between  $\Sigma$  and  $\tilde{\Sigma}^{(k)}$ ). *For any  $k$ ,  $\tilde{\Sigma}^{(k)}$  can be written as*

$$\tilde{\Sigma}^{(k)} = (I - \mathbf{1}\mathbf{e}_k^T) \cdot \Sigma \cdot (I - \mathbf{e}_k\mathbf{1}^T).$$

Conversely, given  $\tilde{\Sigma}^{(k)}$ ’s for all  $k$ ,  $\Sigma$  can be written as

$$\Sigma = \frac{1}{d} \sum_{k=1}^d \tilde{\Sigma}^{(k)} + \frac{1}{d} \text{tr}(\Sigma) \cdot \mathbf{1}\mathbf{1}^T. \quad (2.8)$$

**Remark 2.5.** Given the fact that  $\Sigma \mathbf{1} = 0$ , from (2.8),

$$0 = \mathbf{1}^T \Sigma \mathbf{1} = \frac{1}{d} \sum_{k=1}^d \mathbf{1}^T \tilde{\Sigma}^{(k)} \mathbf{1} + \frac{1}{d} \text{tr}(\Sigma) \cdot \mathbf{1}^T \mathbf{1} \mathbf{1}^T \mathbf{1} = \frac{1}{d} \sum_{k=1}^d \mathbf{1}^T \tilde{\Sigma}^{(k)} \mathbf{1} + \frac{1}{d} \text{tr}(\Sigma) \cdot d^2.$$

Therefore  $\Sigma$  can be derived from  $\tilde{\Sigma}^{(k)}$ 's by

$$\Sigma = \frac{1}{d} \sum_{k=1}^d \tilde{\Sigma}^{(k)} - \frac{1}{d^3} \left( \sum_{k=1}^d \mathbf{1}^T \tilde{\Sigma}^{(k)} \mathbf{1} \right) \cdot \mathbf{1} \mathbf{1}^T. \quad (2.9)$$

**Proposition 2.6** (Relationship between  $\Sigma$  and  $\Theta$ ). *Let  $\Sigma$  have the eigendecomposition*

$$\Sigma = \sum_{k=1}^d \lambda_k \mathbf{u}_k \mathbf{u}_k^T,$$

where  $\{\lambda_k\}$  is the set of ordered eigenvalues of  $\Sigma$  and  $\{\mathbf{u}_k\}$  is the corresponding set of orthonormal eigenvectors. Then

$$0 = \lambda_1 < \lambda_2 \leq \dots \leq \lambda_d,$$

and

$$\mathbf{u}_1 = \frac{1}{\sqrt{d}} \mathbf{1}.$$

Meanwhile,  $\Theta$  can be written as

$$\Theta = \sum_{k=2}^d \frac{1}{\lambda_k} \mathbf{u}_k \mathbf{u}_k^T.$$

In particular, for any  $M > 0$ ,

$$\left( \Sigma + \frac{M}{d} \mathbf{1} \mathbf{1}^T \right)^{-1} = (\Sigma + M \mathbf{u}_1 \mathbf{u}_1^T)^{-1} = \Theta + \frac{1}{M} \mathbf{u}_1 \mathbf{u}_1^T = \Theta + \frac{1}{dM} \mathbf{1} \mathbf{1}^T.$$

**Remark 2.7.** Hentschel et al. (2022) study the matrix  $\Sigma$  and show that it is the Moore-Penrose inverse of  $\Theta$  such that

$$\lim_{M \rightarrow \infty} (\Sigma + M \mathbf{1} \mathbf{1}^T)^{-1} = \Theta.$$

Proposition 2.6 provides a stronger result with a simpler proof.

**Corollary 2.8** (Parameter space of  $\Sigma$  and  $\Theta$ ). *Let*

$$\mathcal{L} = \{A \in \mathbb{R}^{d \times d} : A \succeq 0, A \mathbf{1} = \mathbf{0}, \text{rank}(A) = d - 1\}.$$

Then any  $\Sigma \in \mathcal{L}$  or  $\Theta \in \mathcal{L}$  characterizes an HR distribution.



### 3 The extreme graphical lasso

In this section, we propose a sparse estimator for the precision matrix  $\Theta$ . As we have seen in Section 2, the HR model can be equivalently parametrized by  $\Gamma$ ,  $\Sigma^{(k)}$ 's,  $\Sigma$ ,  $\Theta^{(k)}$ 's or  $\Theta$ . Among these parameter matrices,  $\Sigma^{(k)}$ 's can be most conveniently estimated from data. Given an HR multivariate Pareto distribution  $\mathbf{Y}$ , Engelke et al. (2015) show that

$$(\log \mathbf{Y}_{-k} - \log(Y_k) \cdot \mathbf{1})|_{Y_k > 1} \sim N(\Gamma_{-k,k}/2, \Sigma^{(k)}). \quad (3.1)$$

Therefore  $\Sigma^{(k)}$ 's can be estimated from the sample covariance matrix of the thresholded transformed observations. We will describe the details of the estimator in Section 5.1. For now, we consider using estimators  $\hat{\Sigma}^{(k)}$ 's to derive an estimator for  $\Theta$ . Since each  $\hat{\Sigma}^{(k)}$  requires different truncation and therefore makes use of different information from the data, it is preferred to utilize the estimators  $\hat{\Sigma}^{(k)}$  for all  $k = 1, \dots, d$ .

A straightforward non-sparse estimator for  $\Theta^{(k)}$  is  $(\hat{\Sigma}^{(k)})^{-1}$ , which can be written as

$$\hat{\Theta}^{(k)} := (\hat{\Sigma}^{(k)})^{-1} = \arg \min_{\Theta^{(k)} \succ 0} \left\{ -\log |\Theta^{(k)}| + \text{tr}(\hat{\Sigma}^{(k)} \Theta^{(k)}) \right\}. \quad (3.2)$$

The right hand side of (3.2) corresponds to a pseudo negative log-likelihood in (3.1), which allows us to interpret  $\hat{\Theta}^{(k)}$  as a pseudo-MLE estimator ('pseudo' as to acknowledge the fact that the mean of the Gaussian distribution is estimated separately using the sample mean and not jointly with the covariance matrix). It can also be viewed as the minimization of a Bregman divergence between the observed and estimated inverse covariance matrix (see, e.g. Ravikumar et al., 2011) and therefore can be interpreted outside the Gaussian context.

Given estimators  $\hat{\Sigma}^{(k)}$  for all  $k$ , we may aggregate (3.2) for all  $k$  and solve for  $\Theta$  to minimize

$$\arg \min_{\Theta \in \mathcal{L}} \sum_{k=1}^d \left\{ -\log |\Theta^{(k)}| + \text{tr}(\hat{\Sigma}^{(k)} \Theta^{(k)}) \right\}, \quad (3.3)$$

where each  $\Theta^{(k)}$  denote the submatrix of  $\Theta$  with the  $k$ -th row and column removed.

Let  $S$  be the estimator of  $\Sigma$  from (2.9) defined as follows:

$$S := \frac{1}{d} \sum_{k=1}^d \hat{\Sigma}^{(k)} - \left( \frac{1}{d^3} \sum_{k=1}^d \mathbf{1}^T \hat{\Sigma}^{(k)} \mathbf{1} \right) \mathbf{1} \mathbf{1}^T, \quad (3.4)$$

where  $\hat{\Sigma}^{(k)}$  denote the estimator for  $\tilde{\Sigma}^{(k)}$  augmented from  $\hat{\Sigma}^{(k)}$ . The following proposition shows that the aggregated negative log-likelihood (3.3) can be written as a negative log-likelihood-like expression of  $\Theta$  using  $S$ .

**Proposition 3.1.** *The following problems have equivalent solutions:*

$$\arg \min_{\Theta \in \mathcal{L}} \sum_{k=1}^d \left\{ -\log |\Theta^{(k)}| + \text{tr}(\hat{\Sigma}^{(k)} \Theta^{(k)}) \right\} = \arg \min_{\Theta \in \mathcal{L}} \{ -\log |\Theta|_+ + \text{tr}(S\Theta) \}. \quad (3.5)$$

Here  $|\cdot|_+$  denote the pseudo-determinant (product of all nonzero eigenvalues) of a matrix.

**Remark 3.2.** Lemma 5.1 of Röttger et al. (2023) motivates the same equivalence as in (3.5), where  $S$  is calculated from a different procedure. They propose to first obtain estimate  $\hat{\Gamma}_k$  from  $\hat{\Sigma}^{(k)}$  via (2.5), average all estimates by  $\hat{\Gamma} = \frac{1}{k} \sum_{k=1}^d \hat{\Gamma}_k$ , then obtain the estimate  $S$  from the aggregated estimator  $\hat{\Gamma}$  via (2.7). The two formulation results in the same estimator  $S$ .

### 3.1 Graphical lasso estimator of $\Theta$

Following Proposition 2.6, write  $\Theta$  in its eigen decomposition form

$$\Theta = \sum_{k=2}^d \frac{1}{\lambda_k} \mathbf{u}_k \mathbf{u}_k^T.$$

Then

$$|\Theta|_+ = \frac{1}{\prod_{k=2}^d \lambda_k}.$$

For any  $M > 0$ ,

$$\left| \Theta + \frac{1}{dM} \mathbf{1}\mathbf{1}^T \right| = \left| \Theta + \frac{1}{M} \mathbf{u}_1 \mathbf{u}_1^T \right| = \frac{1}{M} \cdot \frac{1}{\prod_{k=2}^d \lambda_k} = \frac{1}{M} \cdot |\Theta|_+.$$

Combining with the fact that  $\Theta \cdot \mathbf{1} = \mathbf{0}$  for any  $\Theta \in \mathcal{L}$ , the estimator for  $\Theta$  in (3.5) can also be written as

$$\arg \min_{\Theta \in \mathcal{L}} \left\{ -\log \left| \Theta + \frac{1}{dM} \mathbf{1}\mathbf{1}^T \right| + \text{tr} \left( \left( S + \frac{M}{d} \mathbf{1}\mathbf{1}^T \right) \left( \Theta + \frac{1}{dM} \mathbf{1}\mathbf{1}^T \right) \right) \right\},$$

which is similar to minimizing the Gaussian negative log-likelihood function of  $\Theta^* := \Theta + \frac{1}{dM} \mathbf{1}\mathbf{1}^T$  using covariance estimate  $S^* := S + \frac{M}{d} \mathbf{1}\mathbf{1}^T$ . To impose zero-entries to  $\Theta$ , we impose  $L_1$ -penalties on the absolute entries of  $\Theta$ :

$$\arg \min_{\Theta \in \mathcal{L}} \left\{ -\log \left| \Theta + \frac{1}{dM} \mathbf{1}\mathbf{1}^T \right| + \text{tr} \left( \left( S + \frac{M}{d} \mathbf{1}\mathbf{1}^T \right) \left( \Theta + \frac{1}{dM} \mathbf{1}\mathbf{1}^T \right) \right) + \gamma \sum_{i \neq j} |\Theta_{ij}| \right\}.$$

Unlike from the classical graphical lasso, as  $\gamma$  increases, this will not result in a sparse graph. Intuitively, due to the constraint that  $\sum_{i=1}^d \Theta_{ij} = 0$  for any  $j$ ,  $\Theta_{ij}$  will approach  $-\Theta_{jj}/(d-1)$  as  $\gamma$  increases, not 0. See, for example, Theorem 3.1 of Ying et al. (2020).

To obtain a sparse estimator, we propose to relax the search domain of  $\Theta$  and instead solve the following problem:

$$\hat{\Theta}_{\text{lasso}} := \arg \min_{\Theta + \frac{1}{dM} \mathbf{1}\mathbf{1}^T \succ 0} \left\{ -\log \left| \Theta + \frac{1}{dM} \mathbf{1}\mathbf{1}^T \right| + \text{tr} \left( \left( S + \frac{M}{d} \mathbf{1}\mathbf{1}^T \right) \left( \Theta + \frac{1}{dM} \mathbf{1}\mathbf{1}^T \right) \right) + \gamma \sum_{i \neq j} |\Theta_{ij}| \right\}. \quad (3.6)$$

We term the solution of (3.6) the *extreme graphical lasso estimator* of  $\Theta$ .

In Section 4, we show that under suitable conditions, the extreme graphical lasso is consistent in estimating  $\Theta$  and recovering underlying sparse graph structure, despite the relaxation of the search domain.

### 3.2 Solving the extreme graphical lasso

Denote  $c := \frac{1}{dM}$ ,  $\Theta^* := \Theta + \frac{1}{dM}\mathbf{1}\mathbf{1}$  and  $S^* := S + \frac{M}{d}\mathbf{1}\mathbf{1}^T$ . Then the problem in (3.6) can be reformulated as

$$\arg \min_{\Theta^* \succ 0} \left\{ -\log |\Theta^*| + \text{tr}(S^* \Theta^*) + \gamma \sum_{i \neq j} |\Theta_{ij}^* - c| \right\}.$$

This is similar to the Gaussian graphical lasso problem in (1.1) except that we penalize the off-diagonal entries of  $\Theta^*$  to a positive constant  $c$  instead of 0. Despite the similarity, this problem cannot be solved directly by the state-of-the-art GLASSO algorithm proposed in Friedman et al. (2008). Instead, we modify another block coordinate descent algorithm, the P-GLASSO algorithm, from Mazumder and Hastie (2012). Similar to GLASSO, P-GLASSO is computationally efficient and is guaranteed to converge on a trajectory of positive definite matrices. In Appendix E, we provide the algorithm for the extreme graphical lasso and its convergence properties.

## 4 Theoretical results

In this section, we establish the non-asymptotic and asymptotic theories for the extreme graphical lasso. The goal is to learn the graphical structure for extremes and estimate the non-zero entries of  $\Theta$  simultaneously.

Recall that  $(V, E)$  denotes the set of nodes and edges of the graph. Denote the maximum degree of all nodes as  $D = \max_{1 \leq i \leq d} \sum_{j=1}^d 1_{(i,j) \in E}$ . If the dimension  $d = d_n \rightarrow \infty$  as the sample size  $n \rightarrow \infty$ , we can potentially have  $D \rightarrow \infty$  and  $|E| \rightarrow \infty$ . Nevertheless,  $D = O(d)$  and  $|E| = O(d^2)$  always hold.

We first list the conditions required for learning the graph structure. The first condition concerns the structure of the graph reflected in the true covariance matrix  $\Sigma$ .

**Condition 4.1** (Mutual incoherence). *Given  $M > 0$ , define  $\Omega = \Sigma^* \otimes \Sigma^*$  where  $\Sigma^* = \Sigma + \frac{M}{d}\mathbf{1}\mathbf{1}^T$  and  $\otimes$  is the Kroneker product. We assume that there exists  $0 < \alpha < 1$  such that*

$$||\Omega_{E^c E}(\Omega_{EE})^{-1}||_\infty < 1 - \alpha,$$

where  $\Omega_{EE} \in \mathbb{R}^{|E| \times |E|}$  is the submatrix  $(\Omega_{(i,j),(k,l)})_{(i,j) \in E, (k,l) \in E}$  and  $\Omega_{E^c E}$  is defined similarly.

Condition 4.1, also referred to as the irrerepresentability condition, is comparable with Assumption 1 in Ravikumar et al. (2011). Such a condition is needed for theory regarding lasso-type penalization algorithms.

The second condition concerns the tuning parameter  $\gamma = \gamma_n$ . In order to identify the exact graph structure, the tuning parameter should be neither too high nor too low. A low  $\gamma_n$  will result in non-edges not being penalized to zero while a high  $\gamma_n$  will penalize true edges to zero. A suitable  $\gamma_n$  is related to the estimation error when estimating  $\Sigma$ . In Section 5, we will discuss the (non-)asymptotic properties of the estimator  $S$  defined in (3.4) by handling the estimation error  $\|S - \Sigma\|$ . In this section, we formulate the bounds for  $\gamma_n$  using the estimation error  $\delta_n$  based on the event  $\{\|S - \Sigma\|_\infty \leq \delta_n\}$ .

**Condition 4.2.** Assume that there exists  $0 < \epsilon < 1$ , such that

$$\|S - \Sigma\|_\infty \leq \delta_n \leq \frac{(1 - \epsilon)\epsilon\alpha^2}{D\|\|\Sigma^*\|\|_\infty\|\|\Omega_{EE}^{-1}\|\|_\infty[(1 - \epsilon)\alpha + \|\|\Sigma^*\|\|_\infty^2\|\|\Omega_{EE}^{-1}\|\|_\infty]}.$$

Further, assume that the tuning parameter  $\gamma_n$  satisfies  $\underline{C}_\gamma(\delta_n) \leq \gamma_n \leq \overline{C}_\gamma$ , where

$$\overline{C}_\gamma := \frac{(1 - \epsilon)\alpha(1 - \alpha)}{D\|\|\Sigma^*\|\|_\infty\|\|(\Omega_{EE})^{-1}\|\|_\infty[(1 - \epsilon)\alpha + \|\|\Sigma^*\|\|_\infty^2\|\|(\Omega_{EE})^{-1}\|\|_\infty]}, \quad (4.1)$$

$$\underline{C}_\gamma(\delta_n) := \frac{1 - \alpha}{\epsilon\alpha} \cdot \delta_n. \quad (4.2)$$

Note that the upper bound of  $\delta_n$  ensures  $\underline{C}_\gamma \leq \overline{C}_\gamma$  and thus the existence of a suitable  $\gamma_n$ . In Section 5, we show that our estimator  $S$  satisfies  $\delta_n \xrightarrow{P} 0$  as  $n \rightarrow \infty$ . Therefore, this upper bound assumption is satisfied for sufficiently large  $n$  with high probability.

The following theorem provides the concentration bounds for  $\hat{\Theta}_{lasso}$  for fixed  $n$ . The proof is given in Appendix B.

**Theorem 4.1.** Assume that Conditions 4.1 and 4.2 hold. Denote

$$r_n := \frac{\|\|(\Omega_{EE})^{-1}\|\|_\infty}{1 - \alpha} \cdot \gamma_n. \quad (4.3)$$

Then on the event  $\{\|S - \Sigma\|_\infty \leq \delta_n\}$ , the extreme graphical lasso algorithm specified in (3.6) has a unique solution  $\hat{\Theta}_{lasso}$ . Denote the estimated edges as  $\hat{E} := \{(i, j) : \hat{\Theta}_{lasso,ij} \neq 0\}$ . Then

$$\hat{E} = E$$

and

$$\|\hat{\Theta}_{lasso} - \Theta\|_\infty \leq r_n.$$

Next, we present the asymptotic theory when  $n \rightarrow \infty$ . The following asymptotic result follows immediately from Theorem 4.1.

**Theorem 4.2.** Assume that Condition 4.1 holds. Assume that there exists a sequence  $\delta_n \rightarrow 0$  as  $n \rightarrow \infty$ , such that the covariance matrix estimate  $S$  satisfies

$$P(\|S - \Sigma\|_\infty > \delta_n) \rightarrow 0,$$

and

$$\frac{1}{\delta_n} \min\{\|\Theta_{ij}\|; (i, j) \in E, i \neq j\} \rightarrow \infty.$$

Choose the tuning parameter  $\gamma_n = \underline{C}_\gamma(\delta_n)$  as in (4.2). Then, as  $n \rightarrow \infty$ , with probability tending to 1, the extreme graphical lasso estimator (3.6) has a unique solution  $\hat{\Theta}_{lasso}$ . In addition,

$$P(\hat{E} = E) \rightarrow 1 \quad \text{and} \quad \|\hat{\Theta}_{lasso} - \Theta\|_\infty = O_P(\delta_n).$$

## 5 Applying the extreme graphical lasso

### 5.1 Estimators for $\Sigma^{(k)}$

The standard statistical inference for the HR model relies on the following result. Let  $\mathbf{Y}$  be the multivariate Pareto distribution from an HR model with variogram  $\Gamma$ . Engelke et al. (2015) show that

$$(\log \mathbf{Y}_{-k} - \log(Y_k) \cdot \mathbf{1}) |_{Y_k > 1} \sim N(\Gamma_{-k,k}/2, \Sigma^{(k)}), \quad (5.1)$$

where  $\Gamma_{-k,k}$  is the  $k$ -th column of  $\Gamma$  with the  $k$ -th element removed. Given i.i.d. observations  $\mathbf{X}^i = (X_1^i, \dots, X_d^i)$ ,  $1 \leq i \leq n$ , drawn from  $\mathbf{X}$ , an empirical counterpart of  $(\log \mathbf{Y}_{-k} - \log(Y_k) \cdot \mathbf{1}) |_{Y_k > 1}$  can be constructed as follows. Define the transformed observations

$$\hat{X}_k^i = \frac{1}{1 - \hat{F}_k(X_k^i)},$$

where  $\hat{F}_k(x) = \frac{1}{n+1} \sum_{i=1}^n \mathbb{I}\{X_k^i \leq x\}$  is the empirical distribution function based on  $X_k^i$ 's and  $\mathbb{I}$  is the indicator function. Then  $\hat{\mathbf{X}}^i = (\hat{X}_1^i, \dots, \hat{X}_d^i)$  resembles a sample of  $\tilde{\mathbf{X}} = (\tilde{X}_1, \dots, \tilde{X}_d)$  with  $\tilde{X}_k = \frac{1}{1 - F_k(X_k)}$ , albeit not i.i.d.

Consider an intermediate sequence  $k_n$  such that  $k_n \rightarrow \infty$  and  $k_n/n \rightarrow 0$  as  $n \rightarrow \infty$ . Then as  $n \rightarrow \infty$ ,  $\|\hat{\mathbf{X}}^i\|_\infty > \frac{n}{k_n}$  mimicks the condition  $\|\tilde{\mathbf{X}}\|_\infty > u$  with  $u \rightarrow \infty$ . Therefore,

$$\frac{k_n}{n} \hat{\mathbf{X}}^i \left| \|\hat{\mathbf{X}}^i\|_\infty > \frac{n}{k_n} \right.$$

approximately follows the same distribution as  $\mathbf{Y}$ .

Let  $I = \{i : \|\hat{\mathbf{X}}^i\|_\infty > \frac{n}{k_n}\} =: \{i_1, \dots, i_m\}$ , where  $m = |I|$ , indicating the index set corresponding to  $\|\hat{\mathbf{X}}^i\|_\infty > \frac{n}{k_n}$ . Denote  $\hat{\mathbf{Y}}_j = (\hat{Y}_{i_1}, \dots, \hat{Y}_{i_d}) := \frac{k_n}{n} \hat{\mathbf{X}}^{i_j}$  for all  $j = 1, \dots, m$ . Let

$$\hat{\mathbf{W}}_i^{(k)} = \log \hat{\mathbf{Y}}_{i,-k} - \log(\hat{Y}_{ik}) \cdot \mathbf{1},$$

and  $I_k$  be the index set that  $I_k = \{i : \hat{Y}_{ik} > 1\}$  for each dimension  $k = 1, \dots, d$  such that  $|I_k| = k_n$ . Then  $\Sigma^{(k)}$  can be estimated by

$$\hat{\Sigma}^{(k)} := \frac{1}{k_n} \sum_{i \in I_k} \left( \hat{\mathbf{W}}_i^{(k)} - \frac{1}{k_n} \sum_{i \in I_k} \hat{\mathbf{W}}_i^{(k)} \right) \left( \hat{\mathbf{W}}_i^{(k)} - \frac{1}{k_n} \sum_{i \in I_k} \hat{\mathbf{W}}_i^{(k)} \right)^T, \quad (5.2)$$

which is the sample covariance matrix using  $\hat{\mathbf{W}}_i^{(k)}$  conditional on  $\hat{Y}_{ik} > 1$ .

Theoretically an estimate of  $\Theta$  can be constructed via  $\hat{\Theta}^{(k)} = \left( \hat{\Sigma}^{(k)} \right)^{-1}$ . To achieve sparsity in  $\Theta^{(k)}$ , any sparse inverse covariance matrix estimation technique can be applied here. However, reconstruction of  $\Theta$  from a sparse  $\hat{\Theta}^{(k)}$  does not guarantee sparsity on the omitted  $k$ -th row and column. Engelke et al. (2022) propose to estimate a sparse  $\hat{\Theta}^{(k)}$  for each  $k$  and then to use a majority vote to decide whether or not each entry of  $\Theta$  should be zero. This approach is shown to be effective in recovering the sparse structure of  $\Theta$ , when the number of dimension is at a moderate level. For high dimensional case, tuning  $d$  graphical lasso models can be cumbersome.

## 5.2 Convergence of $S$ to $\Sigma$

Recall  $S$  as an estimator for  $\Sigma$  in (3.4). We first present the assumptions needed for bounding the estimation errors for  $S$ . The assumptions are in line with those needed in Theorem 3 in Engelke et al. (2022).

The following condition is needed regarding the tail behavior of  $\tilde{\mathbf{X}} = (\tilde{X}_1, \dots, \tilde{X}_d)$ .

**Condition 5.1** (Assumption 3, Engelke et al., 2022). *Assume that all marginal distributions of the original random vector  $\mathbf{X}$ ,  $F_1, \dots, F_d$ , are continuous. In addition, there exists  $\xi' > 0$  and  $K' < \infty$  independent of  $d$ , such that for all  $J \subset \{1, \dots, d\}$  with  $|J| \in \{2, 3\}$  and  $q \in (0, 1]$ ,*

$$\sup_{x \in [0, 1]^3} \left| \frac{1}{q} P \left( \bigcap_{i \in J} \left\{ \tilde{X}_i > \frac{1}{qx_i} \right\} \right) - \frac{P \left\{ \bigcap_{i \in J} Y_i > \frac{1}{x_i} \right\}}{P(Y_1 > 1)} \right| \leq K' q^{\xi'}.$$

Condition 5.1 is a standard second order condition quantifying the speed of convergence of the tail distribution of  $\tilde{\mathbf{X}}$  towards the limiting distribution  $\mathbf{Y}$  on bounded sets. It has been imposed in other asymptotic theories in multivariate extreme value statistics, see e.g. Einmahl et al. (2012) and Engelke and Volgushev (2022).

Next, we assume that the variogram in the HR distribution  $\Gamma$  has bounded entries.

**Condition 5.2** (Bounded entries). *Assume that the variogram  $\Gamma$  satisfies that  $0 < \underline{\lambda} < \inf_{i \neq j} \sqrt{\Gamma_{ij}} \leq \sup_{i \neq j} \sqrt{\Gamma_{ij}} < \bar{\lambda}$ , with  $\underline{\lambda}$  and  $\bar{\lambda}$  independent of  $d$ .*

Condition 5.2 implies the boundedness in the density of the exponent measure, see Assumption 2 in Engelke et al. (2022): this condition is required for establishing concentration bounds for estimators of  $\Gamma$ . In addition, this condition implies that for any pair  $(i, j)$  with  $i \neq j$ ,  $X_i$  and  $X_j$  are asymptotically dependent.

Then we have the following proposition. Its proof is postponed to Appendix C.

**Proposition 5.1.** *Assume that Conditions 5.1 and 5.2 hold. Then for any  $\xi < \xi'$ , there exists positive constants  $C_1$ ,  $C_2$  and  $C_3$ , depending on  $\xi$ ,  $\xi'$ ,  $\underline{\lambda}$  and  $\bar{\lambda}$ , independent of  $d$ , such that for any  $\varepsilon \geq \varepsilon_n := C_2 d^3 \exp\{-\frac{C_3 k_n}{(\log n)^8}\}$ ,*

$$P(\|S - \Sigma\|_\infty > \delta_n) \leq \varepsilon, \tag{5.3}$$

where

$$\delta_n = \delta_n(\varepsilon) := C_1 \left\{ \left( \frac{k_n}{n} \right)^\xi \left( \log \left( \frac{k_n}{n} \right) \right)^2 + \frac{1 + \sqrt{\frac{1}{C_3} \log(C_2 d^3 / \varepsilon)}}{\sqrt{k_n}} \right\}.$$

*In addition, assume that  $(\log n)^4 \sqrt{\frac{\log d}{k_n}} \rightarrow 0$  as  $n \rightarrow \infty$ . Then*

$$\|S - \Sigma\|_\infty = O_P \left( \left( \frac{k_n}{n} \right)^\xi \left( \log \left( \frac{k_n}{n} \right) \right)^2 + \sqrt{\frac{\log d}{k_n}} \right), \quad n \rightarrow \infty.$$

We remark that this proposition does not require a fixed  $d$  and allows for  $d = d_n \rightarrow \infty$  as  $n \rightarrow \infty$ . Nevertheless, the condition  $(\log n)^4 \sqrt{\frac{\log d}{k_n}} \rightarrow 0$  as  $n \rightarrow \infty$  provides an upper bound for the diverging speed of  $d_n$  towards infinity. It depends not only on  $n$  but also on the intermediate sequence  $k_n$ . Combining Theorem 4.2 and Proposition 5.1, we immediately obtain the speed convergence of the extreme graphical lasso estimator  $\hat{\Theta}_{lasso}$ .

### 5.3 Choice of $M$ : a theoretical guidance

In this section, we provide reasoning for choosing  $M$  in practice. We recommend to choose  $M$  from the interval  $M \in [\lambda_2, \lambda_d]$ , where  $\lambda_2$  and  $\lambda_d$  are the smallest and the largest positive eigenvalues of  $\Sigma$ . Recall from Proposition 2.6 that

$$\Sigma = \sum_{k=1}^d \lambda_k \mathbf{u}_k \mathbf{u}_k^T,$$

with  $0 = \lambda_1 < \lambda_2 \leq \dots \leq \lambda_d$  and  $\mathbf{u}_1 = \frac{1}{\sqrt{d}} \mathbf{1}$ .

The motivation comes from the following upper bound for the mutual incoherence condition.

**Proposition 5.2.** *The quantity  $|||\Omega_{E^c E}(\Omega_{EE})^{-1}|||_\infty$  in Condition 4.1 can be bounded above by*

$$|||\Omega_{E^c E}(\Omega_{EE})^{-1}|||_\infty \leq \left( |E| \cdot \frac{\lambda_{\max}^2(\Omega) - \lambda_{\min}^2(\Omega)}{\lambda_{\min}^2(\Omega)} \right)^{1/2},$$

where  $\lambda_{\max}(\Omega)$  denotes the largest eigenvalue of  $\Omega$ ,

$$\lambda_{\max}(\Omega) = \max\{\lambda_d^2, M^2\},$$

and  $\lambda_{\min}(\Omega)$  denotes the smallest eigenvalue of  $\Omega$ ,

$$\lambda_{\min}(\Omega) = \min\{\lambda_2^2, M^2\}.$$

From Proposition 5.2, choosing  $M$  smaller than  $\lambda_2$  or larger than  $\lambda_d$  will increase the upper bound for  $|||\Omega_{E^c E}(\Omega_{EE})^{-1}|||_\infty$ . Therefore we recommend the choice of  $M \in [\lambda_2, \lambda_d]$  to minimize this upper bound.

### 5.4 Choosing $M$ : numerical examples

We now investigate two examples of  $d = 4$  and show how the choice of  $M$  affects the mutual incoherence condition  $|||\Omega_{E^c E}(\Omega_{EE})^{-1}|||_\infty$ . Figure 1 shows the graph structures for the two examples, the star graph and the diamond graph. The Mutual Incoherence conditions for these two graphs in the classical graphical lasso setting are studied in Ravikumar et al. (2011).

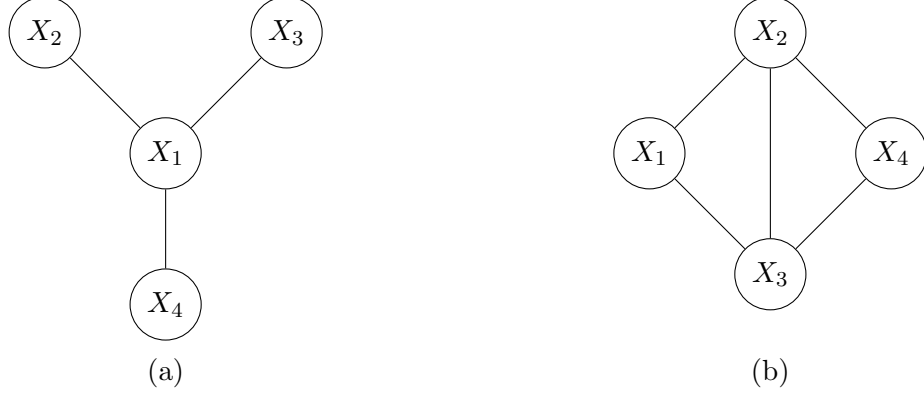


Figure 1: (a) Star graph; (b) Diamond graph.

#### 5.4.1 Star graph

The condition  $\Theta \mathbf{1} = \mathbf{0}$  imposes extra constraints on the precision matrix  $\Theta$ . We consider the following parameterization

$$\Theta = \begin{pmatrix} x+2 & -x & -1 & -1 \\ -x & 2x & 0 & 0 \\ -1 & 0 & 1 & 0 \\ -1 & 0 & 0 & 1 \end{pmatrix}, \quad \text{for some } x > 0$$

which reflects the star graph in Figure 1(a). The top two panels of Figure 2 show the values of  $|||\Omega_{E^c E}(\Omega_{EE})^{-1}|||_\infty$  plotted against the values of  $M$  for star graphs with parameters  $x = 0.8$  and  $x = 1.2$ . As  $[\lambda_2, \lambda_d]$  is suggested as the practical range for  $M$  from Section 5.3, the values of  $\lambda_2$  and  $\lambda_d$  are indicated as dash vertical lines in each graph. We observe that in both examples,  $\lambda_2$  is a good indication of the lowest possible value of  $|||\Omega_{E^c E}(\Omega_{EE})^{-1}|||_\infty$  while the majority of the interval  $M \in [\lambda_2, \lambda_d]$  satisfies the Mutual Incoherence condition.

#### 5.4.2 Diamond graph

Now consider the diamond graph in Figure 1(b) corresponding to the precision matrix

$$\Theta = \begin{pmatrix} x+1 & -x & -1 & 0 \\ -x & x+2 & -1 & -1 \\ -1 & -1 & 3 & -1 \\ 0 & -1 & -1 & 2 \end{pmatrix}, \quad \text{for some } x > 0.$$

We plot the values of  $|||\Omega_{E^c E}(\Omega_{EE})^{-1}|||_\infty$  against the values of  $M$  for parameters  $x = 0.8$  and  $x = 1.2$  on the lower two panels of Figure 2. Again we observe that while  $\lambda_2$  is close the minimum of  $|||\Omega_{E^c E}(\Omega_{EE})^{-1}|||_\infty$ , the interval  $M \in [\lambda_2, \lambda_d]$  in both examples satisfies the Mutual Incoherence condition.



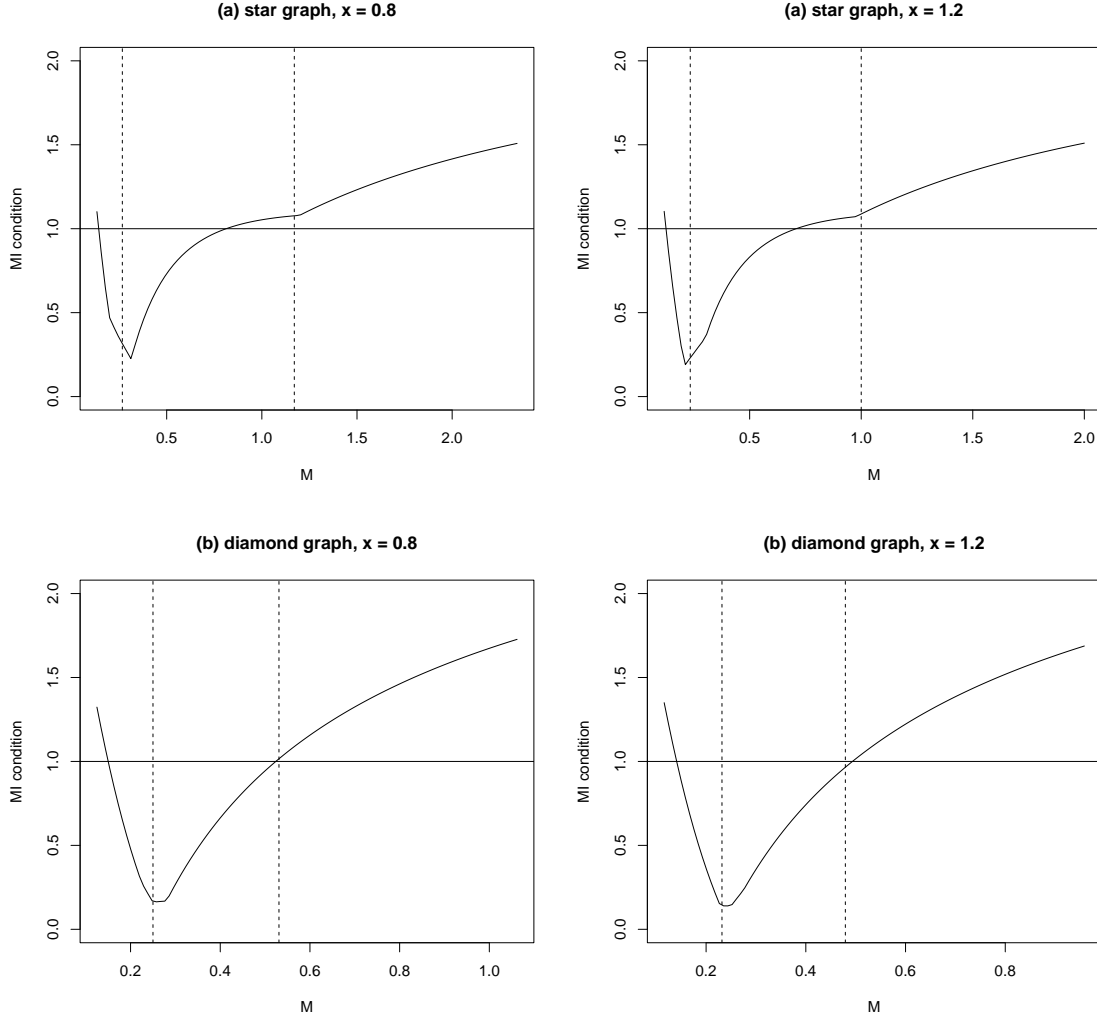


Figure 2: The curves of  $||\Omega_{E^c E}(\Omega_{EE})^{-1}||_\infty$  versus  $M$  for the star graph and the diamond graph, each with parameter values  $x = 0.8$  and  $x = 1.2$ . The two dash vertical lines in each graph indicates the values of  $\lambda_2$  and  $\lambda_d$  for the corresponding  $\Sigma$ .

## 6 Simulations

We conduct a simulation study to show the performance of extreme graphical lasso algorithm. The simulation setup follows closely the one in Engelke et al. (2022), in order to maintain comparability.

### 6.1 Simulation setup

Throughout the simulation study, we sample random graph structures using a preferential attachment model with  $d$  nodes and a degree parameter  $q = 1, 2$ , namely, the Barabasi–Albert model Albert and Barabási (2002), denoted as  $BA(d, q)$ . Note that  $q = 1$  corresponds to a tree model.

For a given graph structure, we sample the precision matrix  $\Theta$  as follows. For each edge in the

graph, we simulate each non-zero upper triangular element in the matrix  $\Theta$  from an independent uniform distribution  $U[-5, -2]$ . The elements in  $\Theta$  corresponding to a non-edge is set to zero and the lower triangular elements are set to mirror their upper triangular counterparts. Finally, the diagonal elements in  $\Theta$  are filled such that each row sum is zero.

We simulate  $n$  observations from the multivariate Pareto distribution as defined in (2.2), where the spectral distribution function follows the HR model corresponding to the simulated precision matrix  $\Theta$ . Here we differ from Engelke et al. (2022) by using the multivariate Pareto distribution instead of the max-stable distribution. For each simulated sample, we follow the procedure in Section 5 to compute the sample covariance matrix  $S$  using an intermediate sequence  $k_n$  and then apply the extreme graphical lasso to estimate the precision matrix  $\Theta$ . The tuning parameter  $M$  is chosen to be  $M = \hat{\lambda}_2$ , where  $\hat{\lambda}_2$  is the estimated second largest eigenvalue of  $S$ , motivated by the theoretical guidance in Section 5.3. For the penalizing parameter  $\gamma_n$ , we tune it in a pre-specified range by minimizing a pseudo-(M)BIC metric defined in Section 6.2. For each setting, we repeat the simulations for  $m = 100$  samples. When evaluating the estimated graph, we use the F1-score defined as follows:

$$\text{F1-Score} = \frac{|E \cap \hat{E}|}{\frac{1}{2} (|E| + |\hat{E}|)},$$

where  $E$  and  $\hat{E}$  are the edge sets for the true and estimated graphs, respectively.

## 6.2 Tuning the penalizing parameter $\gamma_n$

Recall from (5.1) that under the HR model,

$$(\log \mathbf{Y}_{-k} - \log(Y_k) \cdot \mathbf{1}) |_{Y_k > 1} \sim N(\Gamma_{-k,k}/2, \Sigma^{(k)}).$$

The negative log-likelihood based on a pseudo-likelihood can be written as

$$-2 \log L^{(k)} = k_n \left\{ -\log |\Theta^{(k)}| + \text{tr} \left( \hat{\Sigma}^{(k)} \Theta^{(k)} \right) + (d-1) \log(2\pi) \right\},$$

where  $\Theta^{(k)}$  is the partial precision matrix to be estimated,  $\hat{\Sigma}^{(k)}$  is calculated from (5.2) and  $k_n$  is the total number of pseudo observations used in the estimation. We can then define a pseudo-MBIC metric as

$$MBIC^{(k)} = k_n \left\{ -\log |\Theta^{(k)}| + \text{tr} \left( \hat{\Sigma}^{(k)} \Theta^{(k)} \right) \right\} + p^{(k)} (\log \log(d-1)) \log k_n,$$

where  $p^{(k)}$  is the number of non-zero parameters in the non-diagonal part of  $\Theta^{(k)}$  and we omit a constant term in the definition. While MBIC is also used in Engelke et al. (2022), in our case, we base our log-likelihood on the normal distribution instead and avoid evaluating the likelihood of an HR distribution. To maintain comparability, when evaluating a given estimated graphical structure, we re-estimate  $\Theta$  using the original estimated  $\hat{\Sigma}$  matrix and the matrix completion method as in Hentschel et al. (2022) based on the graph estimated by the extreme graphical lasso.

Given  $MBIC^{(k)}$  for  $1 \leq k \leq d$ , we can aggregate them into one metric by either taking the sum or the maximum. We remark that from Proposition 3.1, the sum approach is equivalent to a

pseudo-MBIC metric defined for  $\Theta$  directly. Empirically, both approaches choose the same optimal  $\gamma_n$  in most cases. We opt to use the maximum approach

$$\max MBIC = \max_{1 \leq k \leq d} MBIC^{(k)}.$$

and choose the penalizing parameter  $\gamma_n$  that minimizes  $\max MBIC$ . In such a way, the corresponding estimated graphical structure ensures a goodness-of-fit for all subgraphs.

To demonstrate the tuning procedure, we conduct simulations for  $d = 20$ . We simulate  $m = 100$  samples with  $n = 500$  from the  $BA(d, q)$  model with  $q = 1, 2$ . In the estimation, we choose  $k_n = 75$  corresponding to top 15% of observations. The pre-specified range of  $\gamma_n$  is  $\log_{10}(\gamma_n) \in \{-2, -1.9, -1.8, \dots, 0\}$ , containing 21 values in total. In Figure 3, we plot the average F1 score across these samples when using different values for the penalizing parameter. In addition, we plot the fraction of times when a specific value is chosen as the optimal penalizing parameter following the  $\max MBIC$  standard.

For the  $BA(20, 2)$  model, we observe that the two lines peak at the same value for the penalizing parameter, demonstrating the usefulness of the tuning procedure. For the  $BA(20, 1)$  model, the most selected optimal values tend to be slightly lower than the penalizing parameter value leading to the highest F1 score. This could be due to the fact that the  $BA(20, 1)$  model corresponds to a tree structure. Given that the true graph is a tree, in estimation, a high penalizing parameter may result in an unconnected graph. Due to the evaluation of the log-likelihood, our  $\max MBIC$  standard can only evaluate connected graphs. Therefore we stop the evaluation whenever a graph is unconnected. Consequently, for a more sparse graph such as a tree, the  $\max MBIC$  tuning standard may result in a lower value for the chosen penalizing parameter for the sake of keeping the connectedness.

### 6.3 Graph discovery: large sample

To evaluate the graph recovery performance of the extreme graphical lasso, we perform a large sample simulation with  $d = 20$ . More specifically, we simulate  $m = 100$  samples with  $n = 5000$  from the  $BA(d, q)$  model with  $q = 1, 2$ . For each sample, we choose  $k_n = 500$  corresponding to top 10% of observations to estimate the covariance matrix and then apply the extreme graphical lasso to estimate the graph structure. For tuning the penalizing parameter, we use the same range as in Section 6.2.

Figure 4 shows the aggregated graphs based on aggregating the 100 estimated graphs into one graph, where the thickness of each edge reflects the percentage among the 100 estimated graphs when this pair is identified as an edge. Comparing to the true graph, the extreme graphical lasso algorithm can often identify a true edge. Nevertheless, there are also “false positive” where an estimate edge is not an edge in the true graph. This is particularly the case for the  $BA(d, 1)$  model. Again, we attribute this to the fact that our algorithm aims at maintaining the connectedness of the graph, which often leads to under-penalization.

#### 6.4 Graph discovery: small sample

In this section, we evaluate the performance of the extreme graphical lasso when the sample size is relatively small relative to the dimension.

We simulate  $m = 100$  samples for both  $d = 20$  and  $d = 100$ , from the  $BA(d, q)$  models with  $q = 1, 2$ . For  $q = 1$ , we consider three ratios  $k_n/d \in \{1, 2.5, 5\}$ . For  $q = 2$ , we consider three ratios  $k_n/d \in \{1, 5, 10\}$ . Note that  $k_n/d = 1$  refers to a high dimensional scenario. We simulate  $n = \lceil k_n^{1/0.7} \rceil$  observations for each given  $k_n$ , maintaining  $k_n \approx n^{0.7}$ . After estimating the covariance matrix  $\Sigma$ , we apply the extreme graphical lasso to estimate the graph structure. For tuning the penalizing parameter, we use the same range as in Section 6.2 for  $d = 20$ . To accelerate the calculation for  $d = 100$ , we shrink the range of the tuning parameters to  $\log_{10}(\gamma_n) \in \{-2.1, -2, \dots, -1.7\}$  containing five potential values.

Figure 5 shows the boxplots of the F1 score across each 100 sample for a given setup. For  $d = 20$ , we obtain comparable F1 scores as that of the EGLearn algorithm with graphical lasso method, but worse than that of the EGLearn algorithm with neighborhood selection method, shown in Figure 5 in Engelke et al. (2022). In addition, the F1 scores are higher for higher  $k_n/d$  ratio for the  $BA(20, 2)$  model. For the  $BA(20, 1)$  model, the impact of having a small sample is negligible. For  $d = 100$  and  $q = 2$ , the F1 scores are comparable with that of the EGLearn algorithm with graphical lasso method as in Figure 6 in Engelke et al. (2022). The results for the  $BA(100, 1)$  model worsen. This could be again due to the fact that our tuning procedure is limited by maintaining connectedness. For both  $q = 1$  and  $q = 2$ , we note the deterioration of performance when  $k_n/d$  decreases.

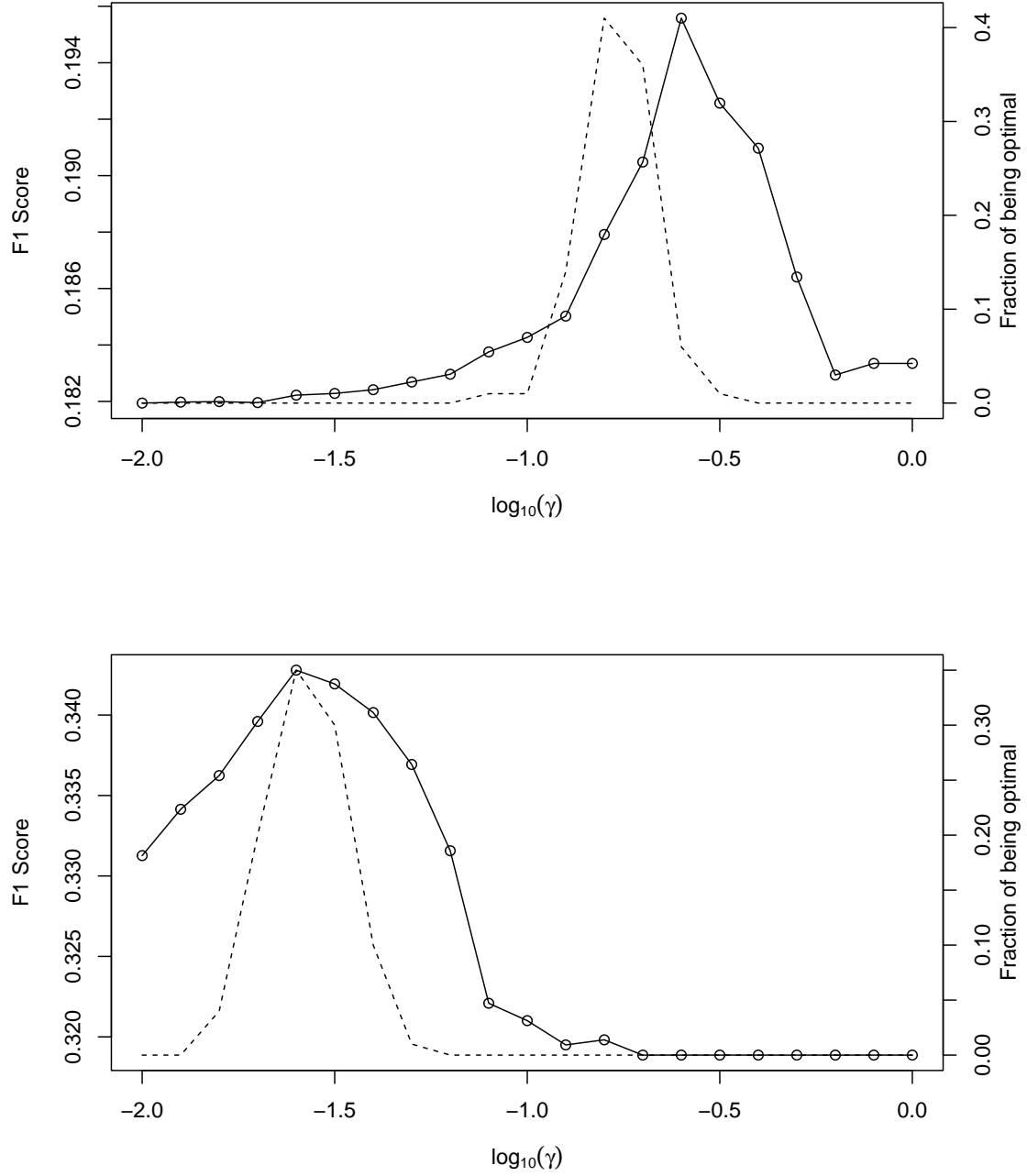


Figure 3: The average F1 score and the fraction of times being optimal versus the penalizing parameter  $\gamma_n$  (in log scale) for the  $BA(20,1)$  (upper panel) and  $BA(20,2)$  (lower panel) graphs. The solid line provides the F1 score for the estimated graphs (left scale). The dash line provides the fraction of times (right scale) when each value is chosen as the optimal penalizing parameter. The plots are over 100 simulated samples.

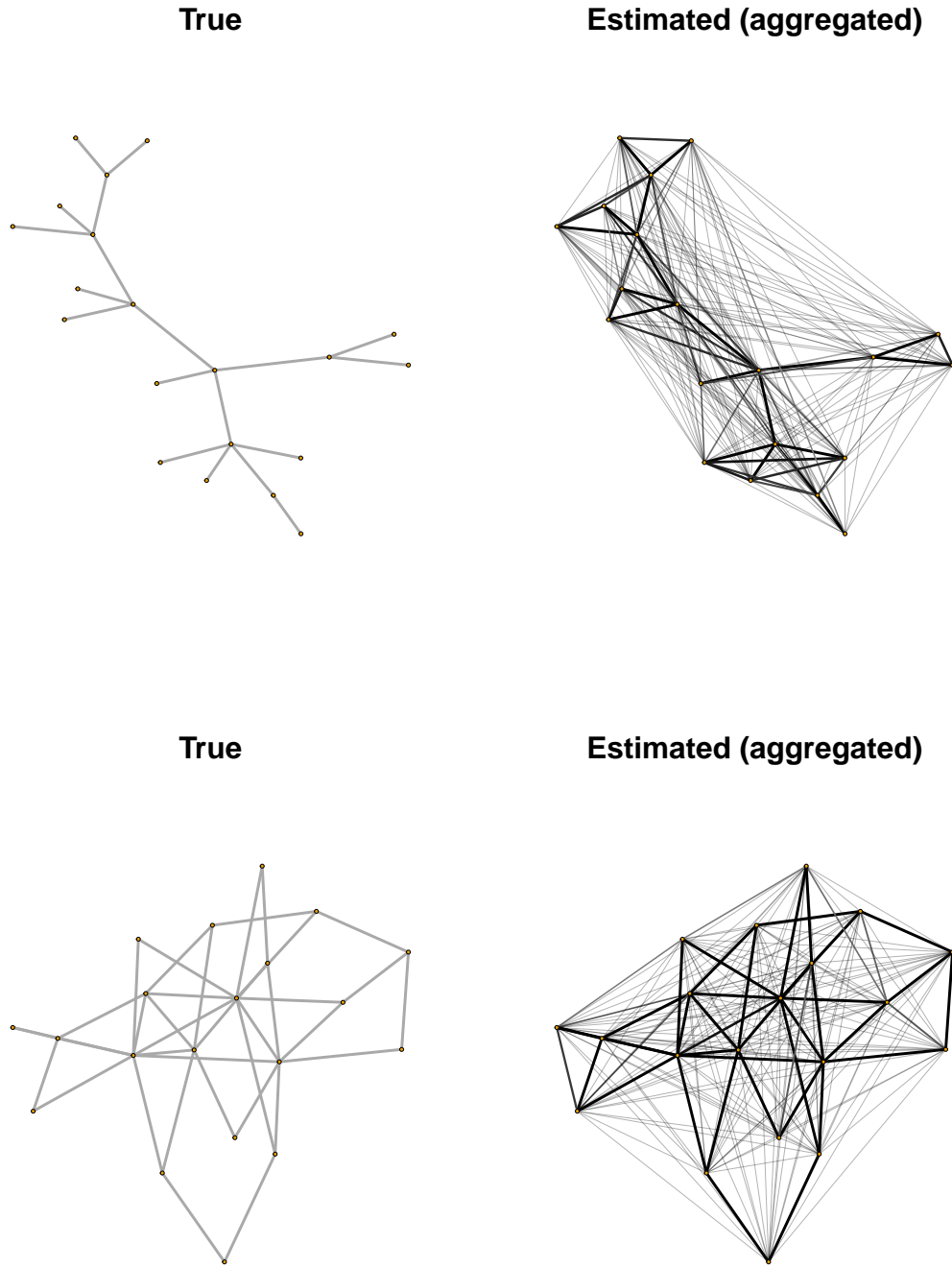


Figure 4: The aggregated graph structure based on 100 simulated samples. The true graph follows the  $BA(20,1)$  (upper panel) and  $BA(20,2)$  (lower panel) model.

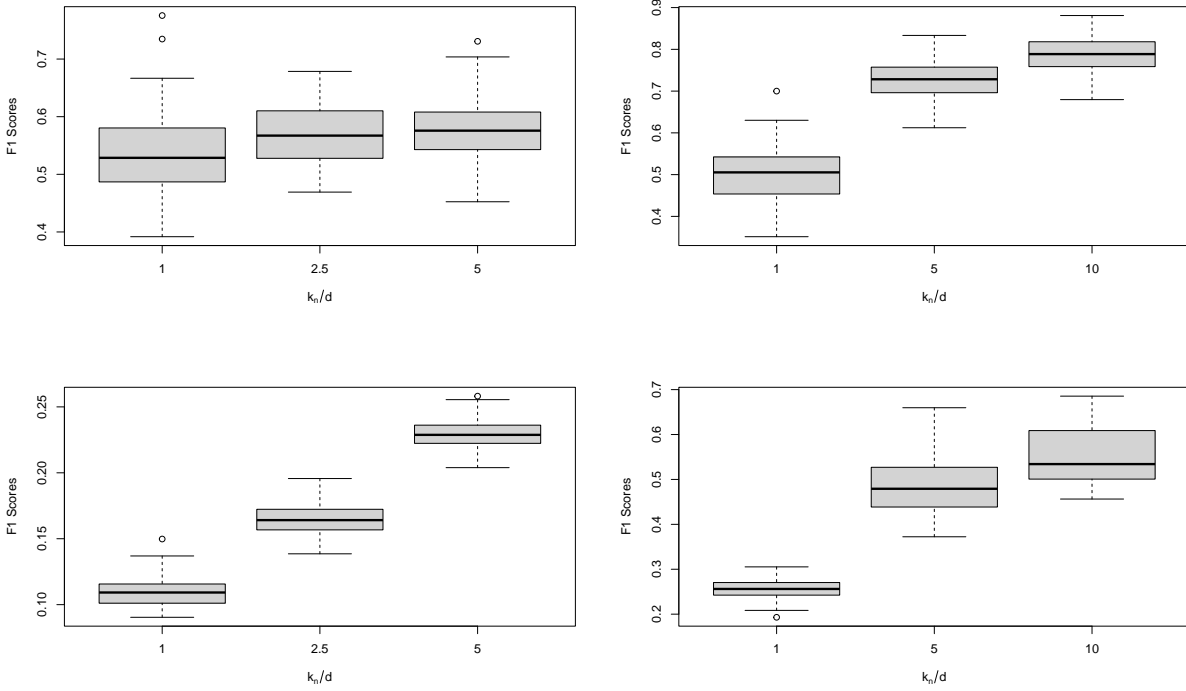


Figure 5: The boxplots for the F1 scores versus different  $k_n/d$  ratios, based on 100 simulated samples. The upper (lower) panel shows the result for  $d = 20$  ( $d = 100$ ). The left (right) graph is based on the  $BA(20, 1)$  ( $BA(20, 2)$ ) model.

## 7 Application

To illustrate the application of the extreme graphical lasso, we apply it to two real data examples.

The first dataset consists of spot foreign exchange rates denominated by the British Pound sterling between 2005 and 2020. The dataset consists of  $n = 3790$  daily observations with  $d = 26$  currencies, preprocessed by taking the absolute values of the de-garched log-returns, see Engelke and Volgushev (2022).

Besides applying the extreme graphical lasso, we also apply the EGLearn with neighborhood selection algorithm as in Engelke et al. (2022). For both algorithms, we use  $k_n = \lceil n^{0.7} \rceil$  for estimating the covariance matrix  $\Sigma$  and the variogram  $\Gamma$ . For estimating the graphical structure, we use the same tuning procedure as in Section 6.1 and use the maxMBIC standard for the extreme graphical lasso. For the EGLearn algorithm, we follow the same tuning procedure as in Engelke et al. (2022).

The upper panels of Figure 6 show the estimated graphs from the two algorithms based on optimally tuned penalizing parameters. Both algorithms identify a large number of edges. In the lower panels of Figure 5, we present an estimated graph from each algorithm using a larger tuning parameter, resulting in sparser graphs that can be easier interpreted and compared. For the EGLearn algorithm, we follow Engelke et al. (2022) to choose  $\rho = 0.53$ . For the extreme graphical lasso algorithm, we choose  $\gamma_n = 0.7$ . Both algorithms reveal that there are two clusters among these currencies, one among Southern Asian countries, the other one among European countries. Observe from the EGLearn algorithm that the two clusters are connected via Japanese Yen, while the extreme graphical lasso results in an isolated node for Japanese Yen.

The second dataset concerns the river discharge at gauging stations from the upper Danube basin. This dataset, as preprocessed in Asadi et al. (2015), consists of  $d = 31$  stations and  $n = 428$  observations. We apply both the EGLearn with neighborhood selection algorithm and the extreme graphical lasso with  $k_n = \lceil n^{0.7} \rceil$ . For the EGLearn algorithm, we use  $\rho = 0.075, 0.2$  and  $0.405$ , following the study of the same dataset in Engelke et al. (2022). For extreme graphical lasso, we use  $\gamma_n = 0.4, 0.44$  and  $0.445$ .

Overall, as the penalizing parameters increase, the EGLearn algorithm inclines to produce more tree-like structure while the EGLasso algorithm produces more cluster structures with disconnected components. We remark that while the river network itself forms a tree network, the river discharge measurements can be influenced by factors other than the geographical locations of the gauging stations. For example, local rainfall or local snowmelt produces dependence in extreme river flow, as detected in the EGLasso algorithm.



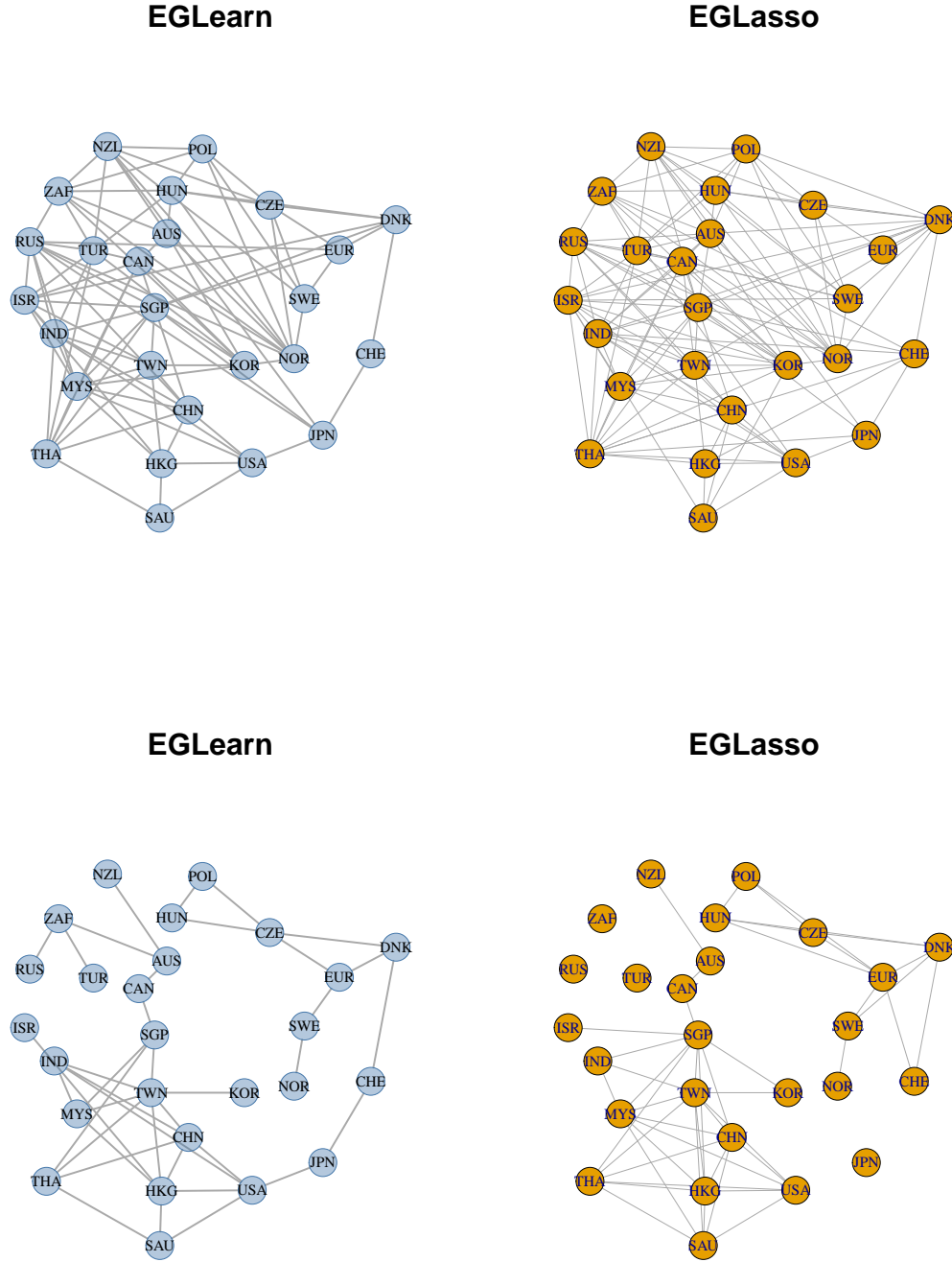


Figure 6: Exchange rate data: identified graphical structures using the EGLearn and extreme graphical lasso (EGLasso) algorithms. The upper panels show the result based on the penalizing parameters turned by optimizing respective MBIC standards. The lower panels show sparser graphs using chosen penalizing parameters:  $\rho = 0.53$  for EGLearn,  $\gamma_n = 0.7$  for EGLasso.

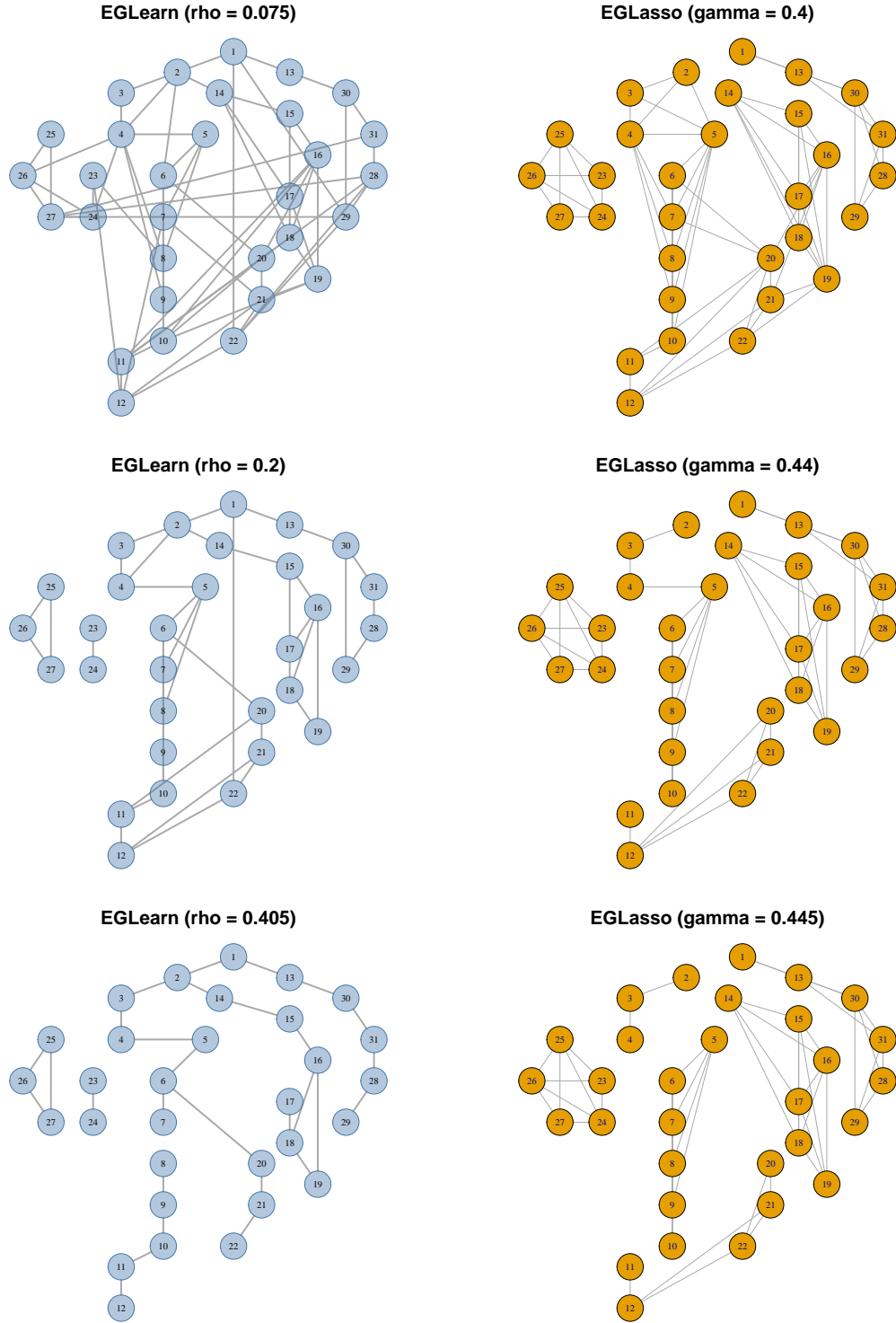


Figure 7: Danube river flow data: identified graphical structures. Left column: the EGLearn algorithm with  $\rho = 0.075, 0.2$  and  $0.405$ . Right column: extreme graphical lasso (EGLasso) algorithms with  $\gamma_n = 0.4, 0.44$  and  $0.445$ .

## Acknowledgements

Phyllis Wan is supported by the Veni grant from the Dutch Research Council (VI.Veni.211E.034). The authors would like to thank the associate editor and two anonymous referees for useful comments, and Frank Röttger and Rutger-Jan Lange for helpful discussions.

## References

- Albert, R. and A.-L. Barabási (2002). Statistical mechanics of complex networks. Reviews of Modern Physics 74(1), 47.
- Asadi, P., A. C. Davison, and S. Engelke (2015). Extremes on river networks. Annals of Applied Statistics 9(4), 2023–2050.
- Banerjee, O., L. El Ghaoui, and A. d’Aspremont (2008). Model selection through sparse maximum likelihood estimation for multivariate gaussian or binary data. Journal of Machine Learning Research 9, 485–516.
- Bertsekas, D. P. (1997). Nonlinear programming. Journal of the Operational Research Society 48(3), 334–334.
- Coles, S. G. and J. A. Tawn (1991). Modelling extreme multivariate events. Journal of the Royal Statistical Society Series B: Statistical Methodology 53, 377–392.
- de Haan, L. and A. Ferreira (2006). Extreme value theory: an introduction. Springer.
- Einmahl, J., A. Krajina, and J. Segers (2012). An M-estimator for tail dependence in arbitrary dimensions. Annals of Statistics 40(3), 1764–1793.
- Engelke, S. and A. Hitz (2020). Graphical models for extremes (with discussion). Journal of the Royal Statistical Society Series B: Statistical Methodology 82, 871–932.
- Engelke, S., M. Lalancette, and S. Volgushev (2022). Learning extremal graphical structures in high dimensions. arXiv preprint arXiv:2111.00840.
- Engelke, S., A. Malinowski, Z. Kabluchko, and M. Schlather (2015). Estimation of Hüsler–Reiss distributions and Brown–Resnick processes. Journal of the Royal Statistical Society Series B: Statistical Methodology 77(1), 239–265.
- Engelke, S. and S. Volgushev (2022). Structure learning for extremal tree models. Journal of the Royal Statistical Society Series B: Statistical Methodology 84(5), 2055–2087.
- Friedman, J., T. Hastie, and R. Tibshirani (2008). Sparse inverse covariance estimation with the graphical lasso. Biostatistics 9, 432–441.

- Hentschel, M., S. Engelke, and J. Segers (2022). Statistical Inference for Hüsler-Reiss Graphical Models Through Matrix Completions. [arXiv preprint arXiv:2210.14292](#).
- Hüsler, J. and R.-D. Reiss (1989). Maxima of normal random vectors: between independence and complete dependence. [Statistics & Probability Letters](#) 7, 283–286.
- Lauritzen, S. L. (1996). [Graphical Models](#). Oxford University Press.
- Mazumder, R. and T. Hastie (2012). The graphical lasso: New insights and alternatives. [Electronic Journal of Statistics](#) 6, 2125.
- Ravikumar, P., M. J. Wainwright, G. Raskutti, and B. Yu (2011). High-dimensional covariance estimation by minimizing l1-penalized log-determinant divergence. [Electronic Journal of Statistics](#) 5, 935–980.
- Rootzén, H. and N. Tajvidi (2006). Multivariate generalized pareto distributions. [Bernoulli](#) 12(5), 917–930.
- Rothman, A. J., P. J. Bickel, E. Levina, and J. Zhu (2008). Sparse permutation invariant covariance estimation. [Electronic Journal of Statistics](#) 2, 494–515.
- Röttger, F., S. Engelke, and P. Zwiernik (2023). Total positivity in multivariate extremes. [The Annals of Statistics](#) 51(3), 962 – 1004.
- Ying, J., J. V. de Miranda Cardoso, and D. Palomar (2020). Nonconvex sparse graph learning under laplacian constrained graphical model. [Advances in Neural Information Processing Systems](#) 33, 7101–7113.
- Yuan, M. and Y. Lin (2007). Model selection and estimation in the gaussian graphical model. [Biometrika](#) 94(1), 19–35.
- Zhou, C. (2010). Are banks too big to fail? measuring systemic importance of financial institutions. [International Journal of Central Banking](#) 6(34), 205–250.

## A Proof of propositions in Sections 2 and 3

*Proof of Proposition 2.1.* Let  $\Gamma$  be the variogram of a random vector  $\mathbf{W}$  with positive definite covariance matrix  $\Sigma$ . Then by definition  $\Gamma$  is symmetric and has diagonal entries 0. From (2.5), we can write

$$\Gamma = \text{diag}(\Sigma) \cdot \mathbf{1}^T + \mathbf{1} \cdot \text{diag}(\Sigma) - 2\Sigma.$$

For any  $\mathbf{x}^T \mathbf{1} = 0$ ,

$$\mathbf{x}^T \Gamma \mathbf{x} = \mathbf{x}^T \text{diag}(\Sigma) \cdot \mathbf{1}^T \mathbf{x} + \mathbf{x}^T \mathbf{1} \cdot \text{diag}(\Sigma) \mathbf{x} - 2\mathbf{x}^T \Sigma \mathbf{x} = -2\mathbf{x}^T \Sigma \mathbf{x} < 0.$$

Therefore  $\Gamma \in \mathcal{D}_0$ .

Conversely, for any  $\Gamma \in \mathcal{D}_0$ , we will construct a positive definite covariance matrix such that the corresponding random vector has variogram  $\Gamma$ . Let

$$\Sigma_k := \Gamma \mathbf{e}_k \mathbf{1}^T + \mathbf{1} \mathbf{e}_k^T \Gamma - \Gamma + \mathbf{e}_k \mathbf{e}_k^T.$$

Any  $\mathbf{y} \in \mathbb{R}^d$  can be written as

$$\mathbf{y} = \mathbf{x} + z \cdot \mathbf{e}_k$$

for some  $z \in \mathbb{R}$  and  $\mathbf{x}^T \mathbf{1} = 0$ . Then

$$\begin{aligned} \mathbf{y}^T \Sigma_k \mathbf{y} &= (\mathbf{x} + z \cdot \mathbf{e}_k)^T (\Gamma \mathbf{e}_k \mathbf{1}^T + \mathbf{1} \mathbf{e}_k^T \Gamma - \Gamma + \mathbf{e}_k \mathbf{e}_k^T) (\mathbf{x} + z \cdot \mathbf{e}_k) \\ &= (\mathbf{x} + z \cdot \mathbf{e}_k)^T (\Gamma \mathbf{e}_k \mathbf{1}^T + \mathbf{1} \mathbf{e}_k^T \Gamma - \Gamma) (\mathbf{x} + z \cdot \mathbf{e}_k) + (\mathbf{e}_k^T (\mathbf{x} + z \cdot \mathbf{e}_k))^2 \\ &= \mathbf{x}^T (\Gamma \mathbf{e}_k \mathbf{1}^T + \mathbf{1} \mathbf{e}_k^T \Gamma - 2\Gamma) \mathbf{x} + z \cdot \mathbf{x}^T (\Gamma \mathbf{e}_k \mathbf{1}^T + \mathbf{1} \mathbf{e}_k^T \Gamma - 2\Gamma) \mathbf{e}_k + \\ &\quad + z \cdot \mathbf{e}_k^T (\Gamma \mathbf{e}_k \mathbf{1}^T + \mathbf{1} \mathbf{e}_k^T \Gamma - 2\Gamma) \mathbf{x} + z^2 \cdot \mathbf{e}_k^T (\Gamma \mathbf{e}_k \mathbf{1}^T + \mathbf{1} \mathbf{e}_k^T \Gamma - 2\Gamma) \mathbf{e}_k + (\mathbf{e}_k^T (\mathbf{x} + z \cdot \mathbf{e}_k))^2 \\ &= -\mathbf{x}^T \Gamma \mathbf{x} + (\mathbf{e}_k^T (\mathbf{x} + z \cdot \mathbf{e}_k))^2 \\ &\geq 0, \end{aligned}$$

where the equality holds if and only if  $\mathbf{x} = \mathbf{0}$  and  $z = 0$ . Therefore  $\Sigma_k$  is a positive definite matrix. It can be shown that

$$\Gamma = \text{diag}(\Sigma) \cdot \mathbf{1}^T + \mathbf{1} \cdot \text{diag}(\Sigma) - 2\Sigma.$$

Therefore  $\Gamma$  is the variogram of a random vector with covariance matrix  $\Sigma_k$ . □

*Proof of Proposition 2.3.* Since  $\sum_{k=1}^d W'_k = \sum_{k=1}^d (W_k - \bar{W}) \equiv 0$ , we have

$$\Sigma \cdot \mathbf{1} = E \left( \sum_{k=1}^d W'_k \cdot \mathbf{W}' \right) = \mathbf{0}.$$

From (2.5), we can write

$$\Gamma = \text{diag}(\Sigma) \cdot \mathbf{1}^T + \mathbf{1} \cdot \text{diag}(\Sigma) - 2\Sigma.$$

Therefore

$$\begin{aligned} & -\frac{1}{2} \left( I - \frac{\mathbf{1}\mathbf{1}^T}{d} \right) \Gamma \left( I - \frac{\mathbf{1}\mathbf{1}^T}{d} \right) \\ &= -\frac{1}{2} \left( I - \frac{\mathbf{1}\mathbf{1}^T}{d} \right) (\text{diag}(\Sigma) \cdot \mathbf{1}^T + \mathbf{1} \cdot \text{diag}(\Sigma) - 2\Sigma) \left( I - \frac{\mathbf{1}\mathbf{1}^T}{d} \right) \\ &= -\frac{1}{2} \left( I - \frac{\mathbf{1}\mathbf{1}^T}{d} \right) \text{diag}(\Sigma) \cdot \mathbf{1}^T \left( I - \frac{\mathbf{1}\mathbf{1}^T}{d} \right) - \frac{1}{2} \left( I - \frac{\mathbf{1}\mathbf{1}^T}{d} \right) \mathbf{1} \cdot \text{diag}(\Sigma) \left( I - \frac{\mathbf{1}\mathbf{1}^T}{d} \right) \\ &\quad + \left( I - \frac{\mathbf{1}\mathbf{1}^T}{d} \right) \Sigma \left( I - \frac{\mathbf{1}\mathbf{1}^T}{d} \right) \\ &= \left( I - \frac{\mathbf{1}\mathbf{1}^T}{d} \right) \Sigma \left( I - \frac{\mathbf{1}\mathbf{1}^T}{d} \right) \\ &= \Sigma, \end{aligned}$$

using the fact that  $\mathbf{1}^T \left( I - \frac{\mathbf{1}\mathbf{1}^T}{d} \right) = 0$  and  $\Sigma \cdot \mathbf{1} = \mathbf{0}$ . □

*Proof of Proposition 2.4.* Let  $\mathbf{W} \sim N(\mathbf{0}, \Sigma)$ . Then  $\Sigma^{(k)}$  is the covariance matrix of

$$\mathbf{W} - W_k \cdot \mathbf{1} = (I - \mathbf{1}\mathbf{e}_k) \cdot \mathbf{W}.$$

From the linear transformation of Gaussian distributions,

$$\tilde{\Sigma}^{(k)} = (I - \mathbf{1}\mathbf{e}_k^T) \cdot \Sigma \cdot (I - \mathbf{1}\mathbf{e}_k^T)^T.$$

For the reverse, we have

$$\begin{aligned} \frac{1}{d} \sum_{k=1}^d \tilde{\Sigma}^{(k)} &= \Sigma - \frac{1}{d} \sum_{k=1}^d \mathbf{1}\mathbf{e}_k^T \Sigma - \frac{1}{d} \sum_{k=1}^d \Sigma \mathbf{e}_k \mathbf{1}^T + \frac{1}{d} \sum_{k=1}^d \mathbf{1}\mathbf{e}_k^T \Sigma \mathbf{e}_k \mathbf{1}^T \\ &= \Sigma - \mathbf{1} \left( \frac{1}{d} \sum_{k=1}^d \mathbf{e}_k \right)^T \Sigma - \Sigma \left( \frac{1}{d} \sum_{k=1}^d \mathbf{e}_k \right) \mathbf{1}^T + \mathbf{1} \left( \frac{1}{d} \sum_{k=1}^d \mathbf{e}_k^T \Sigma \mathbf{e}_k \right) \mathbf{1}^T \\ &= \Sigma - \frac{\mathbf{1}\mathbf{1}^T}{d} \Sigma - \Sigma \frac{\mathbf{1}\mathbf{1}^T}{d} + \mathbf{1} \left( \frac{1}{d} \text{tr}(\Sigma) \right) \mathbf{1}^T \\ &= \Sigma + \frac{1}{d} \text{tr}(\Sigma) \cdot \mathbf{1}\mathbf{1}^T. \end{aligned}$$

Therefore

$$\Sigma = \frac{1}{d} \sum_{k=1}^d \tilde{\Sigma}^{(k)} - \frac{1}{d} \text{tr}(\Sigma) \cdot \mathbf{1}\mathbf{1}^T.$$

□

*Proof of Proposition 2.6.* From  $\Sigma \cdot \mathbf{1} = \mathbf{0}$ , we have that  $\frac{1}{\sqrt{d}} \cdot \mathbf{1}$  is an eigenvector of  $\Sigma$  with eigenvalue 0. Since  $\Sigma$  is positive semidefinite with rank  $d - 1$ , it follows that the rest of the eigenvalues  $\lambda_2 \leq \dots \leq \lambda_d$  must be positive.

Next, we will show that

$$\left( \Sigma + \frac{M}{d} \mathbf{1}\mathbf{1}^T \right) \cdot \left( \Theta + \frac{1}{dM} \mathbf{1}\mathbf{1}^T \right) = I.$$

Note that

$$\tilde{\Sigma}^{(k)} \cdot \Theta = I - \mathbf{e}_k \mathbf{1}^T.$$

(Consider the example of  $k = d$ , where

$$\tilde{\Sigma}^{(d)} \cdot \Theta = \begin{pmatrix} \Sigma^{(d)} & \mathbf{0} \\ \mathbf{0}^T & 0 \end{pmatrix} \cdot \begin{pmatrix} \Theta^{(d)} & \Theta^{(d)} \mathbf{1} \\ \mathbf{1}^T \Theta^{(d)} & \mathbf{1}^T \Theta^{(d)} \mathbf{1} \end{pmatrix} = I - \mathbf{e}_d \mathbf{1}^T.$$

Other cases of  $k$  can be generalized accordingly.) Then from Proposition 2.3,

$$\begin{aligned} \Sigma \cdot \Theta &= \left( \frac{1}{d} \sum_{k=1}^d \tilde{\Sigma}^{(k)} + \frac{1}{d} \text{tr}(\Sigma) \cdot \mathbf{1}\mathbf{1}^T \right) \cdot \Theta \\ &= \frac{1}{d} \sum_{k=1}^d \tilde{\Sigma}^{(k)} \cdot \Theta + \frac{1}{d} \text{tr}(\Sigma) \cdot \mathbf{1}\mathbf{1}^T \cdot \Theta \end{aligned}$$

$$\begin{aligned}
&= \frac{1}{d} \sum_{k=1}^d (I - \mathbf{e}_k \mathbf{1}^T) \\
&= I - \frac{1}{d} \mathbf{1} \mathbf{1}^T.
\end{aligned}$$

Therefore

$$\left( \Sigma + \frac{M}{d} \mathbf{1} \mathbf{1}^T \right) \cdot \left( \Theta + \frac{1}{dM} \mathbf{1} \mathbf{1}^T \right) = \Sigma \cdot \Theta + \frac{M}{d} \mathbf{1} \mathbf{1}^T \cdot \frac{1}{dM} \mathbf{1} \mathbf{1}^T = I - \frac{1}{d} \mathbf{1} \mathbf{1}^T + \frac{1}{d} \mathbf{1} \mathbf{1}^T = I.$$

Now  $\Sigma + \frac{M}{d} \mathbf{1} \mathbf{1}^T$  is positive definite and has the eigendecomposition:

$$\Sigma + \frac{M}{d} \mathbf{1} \mathbf{1}^T = \sum_{k=2}^d \lambda_k \mathbf{u}_k \mathbf{u}_k^T + M \cdot \mathbf{u}_1 \mathbf{u}_1^T.$$

Therefore its inverse as the eigendecomposition:

$$\Theta + \frac{1}{dM} \mathbf{1} \mathbf{1}^T = \sum_{k=2}^d \frac{1}{\lambda_k} \mathbf{u}_k \mathbf{u}_k^T + \frac{1}{M} \cdot \mathbf{u}_1 \mathbf{u}_1^T.$$

It follows that

$$\Theta = \sum_{k=2}^d \frac{1}{\lambda_k} \mathbf{u}_k \mathbf{u}_k^T.$$

And the proposition is proved. □

*Proof of Proposition 3.1.* We proceed to show two results,

$$\frac{1}{d} \sum_{k=1}^d \log |\Theta^{(k)}| = \log |\Theta|_+ + \log(d), \quad (\text{A.1})$$

and

$$\frac{1}{d} \sum_{k=1}^d \text{tr} \left( \hat{\Sigma}^{(k)} \Theta^{(k)} \right) = \text{tr} (S \Theta). \quad (\text{A.2})$$

First consider (A.1). Consider  $d = k$ . We have the following transformation

$$\begin{aligned}
&\begin{pmatrix} I & \mathbf{0} \\ -\mathbf{1}^T & 1 \end{pmatrix} \begin{pmatrix} I & \frac{1}{d} \mathbf{1} \\ \mathbf{0}^T & 1 \end{pmatrix} \begin{pmatrix} \Theta^{(d)} & \mathbf{0} \\ \mathbf{0}^T & d \end{pmatrix} \begin{pmatrix} I & \mathbf{0} \\ \frac{1}{d} \mathbf{1}^T & 1 \end{pmatrix} \begin{pmatrix} I & -\mathbf{1} \\ \mathbf{0}^T & 1 \end{pmatrix} \\
&= \begin{pmatrix} I & \mathbf{0} \\ -\mathbf{1}^T & 1 \end{pmatrix} \begin{pmatrix} \Theta^{(d)} + \frac{1}{d} \mathbf{1} \mathbf{1}^T & \mathbf{1} \\ \mathbf{1}^T & d \end{pmatrix} \begin{pmatrix} I & -\mathbf{1} \\ \mathbf{0}^T & 1 \end{pmatrix} \\
&= \begin{pmatrix} \Theta^{(d)} + \frac{1}{d} \mathbf{1} \mathbf{1}^T & -\Theta^{(d)} \mathbf{1} + \frac{1}{d} \mathbf{1} \\ -\mathbf{1}^T \Theta^{(d)} + \frac{1}{d} \mathbf{1}^T & \mathbf{1}^T \Theta^{(d)} \mathbf{1} + \frac{1}{d} \end{pmatrix} \\
&= \Theta + \frac{1}{d} \mathbf{1} \mathbf{1}^T
\end{aligned}$$

Since

$$\left| \begin{pmatrix} I & \mathbf{0} \\ -\mathbf{1}^T & 1 \end{pmatrix} \right| = \left| \begin{pmatrix} I & \mathbf{0} \\ \frac{1}{d}\mathbf{1}^T & 1 \end{pmatrix} \right| = 1,$$

we have

$$|\Theta|_+ = \left| \Theta + \frac{1}{d}\mathbf{1}\mathbf{1}^T \right| = \left| \begin{pmatrix} \Theta^{(d)} & \mathbf{0} \\ \mathbf{0}^T & d \end{pmatrix} \right| = d|\Theta^{(d)}|.$$

Similarly, we can show that for any  $k$ ,

$$|\Theta|_+ = d|\Theta^{(k)}|.$$

This leads to (A.1).

Now consider (A.2). We have

$$\begin{aligned} \frac{1}{d} \sum_{k=1}^d \text{tr}(\hat{\Sigma}^{(k)} \Theta^{(k)}) &= \text{tr} \left( \left( \frac{1}{d} \sum_{k=1}^d \tilde{\Sigma}^{(k)} \right) \Theta \right) \\ &= \text{tr} \left( \left( \frac{1}{d} \sum_{k=1}^d \tilde{\Sigma}^{(k)} - \left( \frac{1}{d^3} \sum_{k=1}^d \mathbf{1}^T \tilde{\Sigma}^{(k)} \mathbf{1} \right) \mathbf{1}\mathbf{1}^T \right) \Theta \right) \\ &= \text{tr}(S\Theta). \end{aligned}$$

And the proposition is proved. □

## B Proof of Theorem 4.1

*Proof of Theorem 4.1.* The proof is constructed by adapting the proof of Theorem 1 in Ravikumar et al. (2011) to our setting: shrinking the off-diagonal elements to a given constant  $c$ . We point out the differences whenever needed.

We shall focus on the event

$$A = \{\|S - \Sigma\|_\infty < \delta_n\},$$

.

Recall that  $c = \frac{1}{dM}$ ,

$$\Theta^* = \Theta + c\mathbf{1}\mathbf{1}^T,$$

and  $\hat{\Theta}^*$  is the solution to the following graphical lasso problem

$$\hat{\Theta}^* := \arg \min_{\Theta^*} \left\{ -\log |\Theta^*| + \text{tr}(S^* \Theta^*) + \gamma_n \sum_{i \neq j} |\Theta_{ij}^* - c| \right\}$$

and  $\hat{\Theta}_{\text{lasso}} := \hat{\Theta}^* - c\mathbf{1}\mathbf{1}^T$ . The estimated edge set is  $\hat{E} := \{(i, j) : \hat{\Theta}_{\text{lasso}, ij} \neq 0\}$ . We start by proving that on the event  $A$  such a solution exists, is unique and satisfies that,  $\hat{E} \subset E$ , and

$$\|\hat{\Theta}_{\text{lasso}} - \Theta\|_\infty \leq r_n,$$



which is equivalent to proving

$$\|\hat{\Theta}^* - \Theta^*\|_\infty \leq r_n.$$

We first show that the solution  $\hat{\Theta}^*$  exists and is unique. The proof follows the same lines as that for Lemma 3 in Ravikumar et al. (2011). The estimator  $S^*$  is positive definite with all diagonal elements being positive. The rest of the proof follows exactly the same arguments therein.

Next, the solution  $\hat{\Theta}^*$  must satisfy the following KKT condition.

$$-\left(\hat{\Theta}^*\right)^{-1} + S^* + \gamma_n \hat{Z} = 0, \quad (\text{B.1})$$

where

$$\hat{Z}_{ij} = \begin{cases} 0 & \text{if } i = j, \\ \text{sign}(\hat{\Theta}_{ij}^* - c) & \text{if } i \neq j \text{ and } \hat{\Theta}_{ij}^* \neq c, \\ \in [-1, 1] & \text{if } i \neq j \text{ and } \hat{\Theta}_{ij}^* = c. \end{cases}$$

In the following proof, we follow the same idea as in Ravikumar et al. (2011), but adapting that to this modified KKT condition. We shall construct a “witness” precision matrix  $\tilde{\Theta}^*$  as follows. Let  $\tilde{\Theta}^*$  be the solution to the following optimization problem,

$$\tilde{\Theta}^* := \arg \min_{\{\Theta^*: \Theta_{ij}^* = c, (i,j) \in E^c\}} -\log |\Theta^*| + \text{tr}(S^* \Theta^*) + \gamma_n \sum_{i \neq j} |\Theta_{ij}^* - c|. \quad (\text{B.2})$$

This is the same optimization but constrained to a smaller domain. Let  $\tilde{E}$  denote the graph recovered from  $\tilde{\Theta}^*$ . Clearly,  $\tilde{\Theta}^*$  satisfies:  $\tilde{\Theta}_{ij}^* = c$  for  $(i, j) \in E^c$ , i.e.  $\tilde{E} \subset E$ .

We shall show that under the conditions in Theorem 4.1,

- $\tilde{\Theta}^*$  satisfies the above KKT condition;
- $\|\tilde{\Theta}^* - \Theta^*\|_\infty \leq r_n$ .

Then by uniqueness,  $\tilde{\Theta}^* = \hat{\Theta}^*$  which achieves the goal that we are aiming to prove.

With a similar argument regarding the existence and uniqueness of the original optimization problem, the solution to the problem (B.2) also exists and is unique. In addition, it satisfies a similar KKT condition as follows,

$$-\left(\tilde{\Theta}^*\right)_{ij}^{-1} + S_{ij}^* + \gamma_n \tilde{Z}_{ij} = 0, \quad (i, j) \in E,$$

where

$$\tilde{Z}_{ij} = \begin{cases} \text{sign}(\tilde{\Theta}_{ij}^* - c) & \text{if } \tilde{\Theta}_{ij}^* \neq c, \\ \in [-1, 1] & \text{if } \tilde{\Theta}_{ij}^* = c. \end{cases}$$

This coincides with the KKT condition (B.1), but the restrictions are only on entries indexed by  $E$ . As a matter of fact,  $\tilde{Z}$  is only defined on  $E$ . In order to argue  $\tilde{\Theta}^*$  as a candidate for  $\hat{\Theta}^*$  and satisfies the full KKT condition, we will now extend the definition of  $\tilde{Z}$  to  $E^c$  as well.

Define

$$\tilde{Z}_{ij} := \frac{1}{\gamma_n} \left( \left( \tilde{\Theta}^* \right)_{ij}^{-1} - S_{ij}^* \right), \quad (i, j) \notin E.$$

Then the pair  $(\tilde{\Theta}^*, \tilde{Z})$  satisfies the original KKT equation (B.1). What remains to be proved is that  $\tilde{Z}$  also satisfies

$$|\tilde{Z}_{ij}| \leq 1, \quad (i, j) \notin E.$$

To summarize, in order to complete the proof of Theorem 4.1, we will show that on the event  $A$ ,

**Goal 1:**  $|\tilde{Z}_{ij}| \leq 1, \quad (i, j) \notin E.$

**Goal 2:**  $\|\tilde{\Theta}^* - \Theta^*\|_\infty \leq r_n.$

In the rest of the proof we denote

$$\Delta := \tilde{\Theta}^* - \Theta^*.$$

For  $(i, j) \notin E$ ,  $\tilde{\Theta}_{ij} = c$  by definition and  $\Theta_{ij} = c$ . Therefore,  $\Delta_{E^c} = \mathbf{0}$  and **Goal 2** above can be translated to

$$\|\Delta_E\|_\infty \leq r_n.$$

To handle the KKT condition for  $\tilde{\Theta}^*$ , we start with handling  $\left( \tilde{\Theta}^* \right)^{-1}$  as follows:

$$\begin{aligned} \left( \tilde{\Theta}^* \right)^{-1} &= (\Theta^* + \Delta)^{-1} \\ &= (\Theta^*(I + \Sigma^* \Delta))^{-1} \\ &= (I + \Sigma^* \Delta)^{-1} \Sigma^* =: J \Sigma^*. \end{aligned}$$

Now in the case where  $\|\Sigma^* \Delta\|_\infty < 1$ , we can expand  $J$  as

$$J = \sum_{k=0}^{\infty} (-1)^k (\Sigma^* \Delta)^k = I - \Sigma^* \Delta + (\Sigma^* \Delta)^2 J.$$

Inspired from this relation, we can use  $\Sigma^* - \Sigma^* \Delta \Sigma^*$  to approximate  $\left( \tilde{\Theta}^* \right)^{-1}$  and define

$$R := \left( \tilde{\Theta}^* \right)^{-1} - (\Sigma^* - \Sigma^* \Delta \Sigma^*),$$

as the approximation error. Here  $R$  is defined regardless of whether  $\|\Sigma^* \Delta\|_\infty < 1$ .

Recall that  $\Sigma^* = \Sigma + \frac{M}{d} \mathbf{1} \mathbf{1}^T$  and  $S^* = S + \frac{M}{d} \mathbf{1} \mathbf{1}^T$ . Define

$$R' := S^* - \Sigma^* = S - \Sigma.$$

On the event  $A$ , we have that  $\|R'\|_\infty \leq \delta_n$ .

Rewrite the KKT condition as

$$\Sigma^* \Delta \Sigma^* - R + R' + \gamma_n \tilde{Z} = 0.$$

We vectorize it using the notation  $\bar{\cdot}$  as the vectorization of a matrix. Then the vectorized KKT condition is

$$\overline{\Sigma^* \Delta \Sigma^*} - \overline{R} + \overline{R'} + \gamma_n \overline{\tilde{Z}} = 0.$$

Note that

$$\overline{\Sigma^* \Delta \Sigma^*} = (\Sigma^* \otimes \Sigma^*) \overline{\Delta} =: \Omega \overline{\Delta},$$

where  $\Omega := \Sigma^* \otimes \Sigma^*$  denotes the Kronecker product of  $\Sigma^*$  with itself. Then we have

$$\Omega \overline{\Delta} - \overline{R} + \overline{R'} + \gamma_n \overline{\tilde{Z}} = 0.$$

By examining the rows of  $\Omega$  indexed by  $E$  and  $E^c$  separately and noting that  $\Delta_{E^c} = 0$ , we get

$$\Omega_{EE} \overline{\Delta}_E - \overline{R}_E + \overline{R'}_E + \gamma_n \overline{\tilde{Z}}_E = 0, \quad (\text{B.3})$$

$$\Omega_{E^c E} \overline{\Delta}_E - \overline{R}_{E^c} + \overline{R'}_{E^c} + \gamma_n \overline{\tilde{Z}}_{E^c} = 0. \quad (\text{B.4})$$

## Proof of Goal 2

To prove Goal 2, we shall show that for any pre-specified  $\|\tilde{Z}_E\|_\infty \leq 1$ , there exists a solution to  $\Delta$  which satisfies:

- $-(\Theta^* + \Delta)_E^{-1} + S_E^* + \gamma_n \tilde{Z}_E = 0$ ;
- $\Delta_{E^c} = 0$ ;
- $\|\Delta_E\|_\infty \leq r_n$ .

With the statement above proven, given the  $\tilde{Z}_E$  produced from the KKT condition for  $\tilde{\Theta}^*$ , a solution  $\Delta$  exists and coincides with  $\tilde{Z}_E$ . Then this is the unique solution. Hence  $\|\tilde{\Theta}^* - \Theta^*\|_\infty \leq r_n$  which concludes **Goal 2**.

Now we construct such a solution  $\Delta$ . Recall that  $\Delta_{E^c} = \mathbf{0}$ , we only need to construct a suitable  $\Delta_E$  by utilizing the Brouwer fixed point theorem.

The solution  $\Delta_E$  satisfies (B.3), which can be rewritten as

$$\overline{\Delta}_E = (\Omega_{EE})^{-1} \left( \overline{R}_E - \overline{R'}_E - \gamma_n \overline{\tilde{Z}}_E \right).$$

We regard

$$R = \left( \tilde{\Theta}^* \right)^{-1} - (\Sigma^* - \Sigma^* \Delta \Sigma^*)$$

as a function of  $\Delta$  or eventually a function of  $\overline{\Delta}_E$ . To stress this point we define it as  $R = R(\overline{\Delta}_E)$ . Also recall that  $R' = S^* - \Sigma^*$  does not depend on  $\overline{\Delta}_E$ . Then we can write the above equation as

$$\overline{\Delta}_E = (\Omega_{EE})^{-1} \left( \overline{R}_E(\overline{\Delta}_E) - \overline{R'}_E - \gamma_n \overline{\tilde{Z}}_E \right) := F(\overline{\Delta}_E).$$

Consider the closed ball  $B(r_n) := \{x \in \mathbb{R}^{|E|} : \|x\|_\infty \leq r_n\}$ . If  $F$  is a continuous mapping from  $B(r_n)$  onto itself, then there exists a fixed point  $\overline{\Delta}_E$  on  $B(r_n)$  such that  $\overline{\Delta}_E = F(\overline{\Delta}_E)$  following the Brouwer fixed point theorem. This is exactly the desired solution.

In the proof of Theorem 1 in Ravikumar et al. (2011), a similar mapping  $F$  was defined and claimed to be “clearly continuous”. In fact, the continuity requires more conditions. Here we provide a careful argument for the continuity.

While most terms in the definition of  $F$  are continuous functions, the term  $\bar{\tilde{Z}}_E$  is related to  $\bar{\Delta}_E$  by  $\tilde{Z}_E = \text{sign}(\tilde{\Theta}_E^* - c) = \text{sign}(\Delta_E + \Theta_E^* - c)$ , which is a potentially discontinuous function, due to the discontinuity of the sign function. Nevertheless, with assuming that  $\min\{\|\Theta_{ij}\|; (i, j) \in E, i \neq j\} > r_n$ , since  $\|\Delta_E\| \leq r_n$ , we have  $\tilde{Z}_E = \text{sign}(\Delta_E + \Theta_E^* - c) = \text{sign}(\Theta_E)$ , which is not related to  $\Delta_E$ . Then  $F$  defined above is a continuous mapping.

Next, we need to show that  $F$  projects  $B(r_n)$  onto itself, that is, for any  $\bar{\Delta}_E$  satisfying  $\|\bar{\Delta}_E\|_\infty \leq r_n$ , we have  $\|F(\bar{\Delta}_E)\|_\infty \leq r_n$ . For any  $\|\bar{\Delta}_E\|_\infty \leq r_n$ , we write

$$\|F(\bar{\Delta}_E)\|_\infty \leq \|(\Omega_{EE})^{-1}\|_\infty \left( \|R\|_\infty + \|R'\|_\infty + \gamma_n \|\bar{\tilde{Z}}_E\|_\infty \right) \leq \|(\Omega_{EE})^{-1}\|_\infty (\|R\|_\infty + \|R'\|_\infty + \gamma_n),$$

due to the fact that  $\|\bar{\tilde{Z}}_E\|_\infty \leq 1$

We first handle  $\|R\|_\infty$ . Recall that

$$R := (\tilde{\Theta}^*)^{-1} - (\Sigma^* - \Sigma^* \Delta \Sigma^*) = \sum_{k=2}^{\infty} (-1)^k (\Sigma^* \Delta)^k \Sigma^* = (\Sigma^* \Delta)^2 J \Sigma^*,$$

where

$$J = (I + \Sigma^* \Delta)^{-1} = \sum_{k=0}^{\infty} (-1)^k (\Sigma^* \Delta)^k,$$

provided that  $\|\Sigma^* \Delta\|_\infty < 1$ . To ensure this condition,

$$\|\Sigma^* \Delta\|_\infty = \|\Sigma^* (\tilde{\Theta} - \Theta)\|_\infty \leq D \|\Sigma^*\|_\infty \cdot r_n,$$

where  $D$  is the maximum degree in the graph. Therefore  $\|\Sigma^* \Delta\|_\infty < 1$  holds by requiring that

$$D \|\Sigma^*\|_\infty \cdot r_n \leq C_4 < 1. \quad (\text{B.5})$$

The upper bound  $C_4$  implies that  $\|J^T\|_\infty \leq \frac{1}{1-C_4}$ .

With the condition (B.5), we can further derive an upper bound for  $\|R\|_\infty$ . Consider one specific element in  $R$ . With denoting  $\mathbf{e}_i$  as a vector with all zero elements except a one element at the  $i$ -th dimension, we have that

$$R_{ij} = \mathbf{e}_i^T (\Sigma^* \Delta)^2 J \Sigma^* \mathbf{e}_j \leq \|\mathbf{e}_i^T (\Sigma^* \Delta)^2\|_\infty \|J \Sigma^* \mathbf{e}_j\|_1 \leq \|(\Sigma^* \Delta)^2\|_\infty \|\Sigma^* J^T\|_\infty.$$

By considering all possible  $(i, j)$  we get that,

$$\begin{aligned} \|R\|_\infty &\leq \|(\Sigma^* \Delta)^2\|_\infty \|\Sigma^* J^T\|_\infty \\ &\leq \|\Sigma^* \Delta\|_\infty \|\Sigma^* \Delta\|_\infty \|J^T\|_\infty \|\Sigma^*\|_\infty \\ &\leq D \|\Sigma^*\|_\infty \cdot r_n \cdot \|\Sigma^*\|_\infty r_n \cdot \frac{1}{1-C_4} \cdot \|\Sigma^*\|_\infty \\ &< C_5 \cdot r_n^2, \end{aligned}$$

where  $C_5 = \frac{D}{1-C_4} |||\Sigma^*|||_\infty^3$ .

Next, since  $R' = S^* - \Sigma^* = S - \Sigma$ , we have that on the event  $A$ ,  $\|R'\|_\infty \leq \delta_n$ . Combining the upper bounds for  $\|R\|_\infty$  and  $\|R'\|_\infty$ , we get that,

$$\|F(\Delta_E)\|_\infty \leq |||(\Omega_{EE})^{-1}|||_\infty (C_5 \cdot r_n^2 + \delta_n + \gamma_n) \leq r_n,$$

by requiring that

$$C_5 \cdot r_n^2 + \delta_n + \gamma_n \leq \frac{1}{|||(\Omega_{EE})^{-1}|||_\infty} \cdot r_n \quad (\text{B.6})$$

If the two required conditions (B.5) and (B.6) hold, we achieve **Goal 2** by utilizing the Brouwer fixed point theorem.

## Proof of Goal 1

To prove **Goal 1**, we shall show that with the constructed solution above, we have

$$\|\bar{\bar{Z}}_{E^c}\|_\infty \leq 1.$$

We rewrite the equation (B.4) as

$$\bar{\bar{Z}}_{E^c} = -\frac{1}{\gamma_n} \Omega_{EE^c} \bar{\Delta}_E + \frac{1}{\gamma_n} \bar{R}_{E^c} - \frac{1}{\gamma_n} \bar{R}'_{E^c},$$

and the substitute  $\bar{\Delta}_E$  above using (B.3) to get that

$$\bar{\bar{Z}}_{E^c} = -\frac{1}{\gamma_n} \Omega_{EE^c} (\Omega_{EE})^{-1} \left( -\bar{R}_E + \bar{R}'_E + \gamma_n \bar{\bar{Z}}_E \right) + \frac{1}{\gamma_n} \bar{R}_{E^c} - \frac{1}{\gamma_n} \bar{R}'_{E^c}.$$

The upper bound for  $\|\bar{\bar{Z}}_{E^c}\|_\infty$  is then

$$\|\bar{\bar{Z}}_{E^c}\|_\infty \leq \frac{1}{\gamma_n} |||\Omega_{EE^c} (\Omega_{EE})^{-1}|||_\infty \left( \|R\|_\infty + \|R'\|_\infty + \gamma_n \|\bar{\bar{Z}}_E\|_\infty \right) + \frac{1}{\gamma_n} \|R\|_\infty + \frac{1}{\gamma_n} \|R'\|_\infty.$$

Using the same upper bounds derived in the proof of **Goal 2**, we have

$$\begin{aligned} \|\bar{\bar{Z}}_{E^c}\|_\infty &\leq \frac{1}{\gamma_n} |||\Omega_{EE^c} (\Omega_{EE})^{-1}|||_\infty (\delta_n + C_5 \cdot r_n^2 + \gamma_n) + \frac{1}{\gamma_n} (\delta_n + C_5 \cdot r_n^2) \\ &= |||\Omega_{EE^c} (\Omega_{EE})^{-1}|||_\infty + \frac{1}{\gamma_n} (|||\Omega_{EE^c} (\Omega_{EE})^{-1}|||_\infty + 1) (\delta_n + C_5 \cdot r_n^2). \end{aligned}$$

Since Condition (4.1) ensures that  $|||\Omega_{EE^c} (\Omega_{EE})^{-1}|||_\infty < 1 - \alpha$ , To satisfy  $\|\bar{\bar{Z}}_{E^c}\|_\infty \leq 1$ , we only need to further require

$$\delta_n + C_5 \cdot r_n^2 \leq \frac{\alpha}{1 - \alpha} \gamma_n. \quad (\text{B.7})$$

To conclude, the theorem is proven provided that the three conditions (B.5)–(B.7) hold. The last step is to verify these three relations under the conditions in Theorem 4.1.

Recall that  $r_n$  is defined in (4.3)

$$r_n := \frac{|||(\Omega_{EE})^{-1}|||_\infty}{1 - \alpha} \cdot \gamma_n.$$

Clearly, this definition together with (B.7) implies (B.6). Hence we only need to verify the conditions (B.5) and (B.7).

We write the two conditions in terms of  $\delta_n$  and  $\gamma_n$ :

$$\begin{aligned} D|||\Sigma^*|||_\infty \frac{|||(\Omega_{EE})^{-1}|||_\infty}{1-\alpha} \cdot \gamma_n &\leq C_4 \\ \delta_n + \frac{D}{1-C_4} |||\Sigma^*|||_\infty^3 \cdot \left( \frac{|||(\Omega_{EE})^{-1}|||_\infty}{1-\alpha} \right)^2 \cdot \gamma_n^2 &\leq \frac{\alpha}{1-\alpha} \cdot \gamma_n. \end{aligned}$$

where  $C_5$  is substituted by  $\frac{D}{1-C_4} |||\Sigma^*|||_\infty^3$ :

The lower bound for  $\gamma_n$  in (4.2) ensures that  $\delta_n \leq \epsilon \frac{\alpha}{1-\alpha} \gamma_n$  for some  $0 < \epsilon < 1$ , we thus need to require that

$$\frac{D}{1-C_4} |||\Sigma^*|||_\infty^3 \cdot \left( \frac{|||(\Omega_{EE})^{-1}|||_\infty}{1-\alpha} \right)^2 \cdot \gamma_n \leq (1-\epsilon) \frac{\alpha}{1-\alpha},$$

which guarantees the second condition. Together with the first condition, we have obtained an upper bound for  $\gamma_n$  as

$$\gamma_n \leq \min \left\{ \frac{C_4(1-\alpha)}{D|||\Sigma^*|||_\infty |||(\Omega_{EE})^{-1}|||_\infty}, \frac{(1-C_4)(1-\epsilon)\alpha(1-\alpha)}{D|||\Sigma^*|||_\infty^3 |||(\Omega_{EE})^{-1}|||_\infty^2} \right\}.$$

We choose  $C_4$  such that the two terms in the minimum are equal. That is

$$C_4 = \frac{(1-\epsilon)\alpha}{(1-\epsilon)\alpha + |||\Sigma^*|||_\infty^2 |||(\Omega_{EE})^{-1}|||_\infty} < 1,$$

which leads to

$$\gamma_n \leq \frac{(1-\epsilon)\alpha(1-\alpha)}{D|||\Sigma^*|||_\infty |||(\Omega_{EE})^{-1}|||_\infty [(1-\epsilon)\alpha + |||\Sigma^*|||_\infty^2 |||(\Omega_{EE})^{-1}|||_\infty]}.$$

This is exactly the required upper bound for  $\gamma_n$  in (4.1). □

## C Proof of Proposition 5.1

*Proof of Proposition 5.1.* We intend to apply Theorem 3 in Engelke et al. (2022). For that purpose, we first verify all assumptions needed for that theorem, namely Assumptions 1 and 2 therein.

We handle Assumption 1 first. Based on Lemma S3 in Engelke et al. (2022), Condition 5.2 implies that for any  $\xi'' > 0$ , there exists  $K_{\xi''} > 0$  depending on  $\underline{\lambda}$  and  $\bar{\lambda}$ , but independent of  $d$ , such that Assumption 4 therein holds. Denote  $K = K' + 2K_{\xi''}$  and  $\xi = \xi' \xi'' / (1 + \xi' + \xi'')$ . Together with Condition 5.1, we get that Assumption 1 in Engelke et al. (2022) holds. In particular, one can choose  $\xi''$  sufficiently large such that  $\xi$  can be any constant satisfying  $\xi < \xi'$ .

Next, Assumption 2 in Engelke et al. (2022) holds automatically for all non-degenerate HR distribution satisfying our Condition 5.2. Therefore, we can then apply Theorem 3 therein to

obtain that there exists positive constants  $C_1$ ,  $C_2$  and  $C_3$ , independent of  $d$ , such that for any  $k_n \geq n^\xi$  and  $\lambda \leq \sqrt{k_n}/(\log n)^4$ ,

$$P\left(\max_{1 \leq k \leq d} \|\hat{\Sigma}^{(k)} - \Sigma^{(k)}\|_\infty > C_1 \left\{ \left(\frac{k_n}{n}\right)^\xi \left(\log\left(\frac{k_n}{n}\right)\right)^2 + \frac{1+\lambda}{\sqrt{k_n}} \right\}\right) \leq C_2 d^3 e^{-C_3 \lambda^2}. \quad (\text{C.1})$$

The constant  $C_1$  here equals to  $\frac{3}{2}\bar{C}$  in Theorem 3 in Engelke et al. (2022) because we are estimating the matrix  $\Sigma$  instead of the variogram  $\Gamma$ .

For any  $\varepsilon \geq C_2 d^3 \exp\{-\frac{C_3 k_n}{(\log n)^8}\}$ , one can choose  $\lambda = \sqrt{\frac{1}{C_3} \log(C_2 d^3/\varepsilon)} \leq \frac{\sqrt{k_n}}{(\log n)^4}$  in (C.1) to obtain the element-wise bound for the estimation error  $\hat{\Sigma}^{(k)} - \Sigma^{(k)}$  uniformly for all  $1 \leq k \leq d$ .

Since

$$S - \Sigma = \frac{1}{d} \sum_{k=1}^d (\hat{\Sigma}^{(k)} - \Sigma^{(k)}) - \frac{1}{d} \sum_{k=1}^d \left( \frac{1}{d^2} \mathbf{1}^T (\hat{\Sigma}^{(k)} - \Sigma^{(k)}) \mathbf{1} \right) \mathbf{1} \mathbf{1}^T,$$

which implies that  $\|S - \Sigma\|_\infty \leq 2 \max_{1 \leq k \leq d} \|\hat{\Sigma}^{(k)} - \Sigma^{(k)}\|_\infty$ , we immediately get the inequality (5.3) with replacing  $C_1$  by  $2C_1$ . W.l.o.g., we continue using  $C_1$ .

For the asymptotic statement, if  $(\log n)^4 \sqrt{\frac{\log d}{k_n}} \rightarrow 0$  as  $n \rightarrow \infty$ , then the lower bound for  $\varepsilon$ ,  $\varepsilon_n \rightarrow 0$  as  $n \rightarrow \infty$ . In other words, for any  $\varepsilon > 0$ , with sufficiently large  $n$ ,  $\varepsilon > \varepsilon_n$  holds. The asymptotic statement follows immediately.  $\square$

## D Proof of Proposition 5.2

To prove Proposition 5.2, we require the following lemma.

**Lemma D.1.** *Let  $A \in \mathbb{R}^{p \times p}$  be a symmetric square matrix and let  $A_{EE}$  be a principal sub-matrix of  $A$  obtained by only keeping the columns and rows indexed by  $E \subset \{1, \dots, p\}$ . Then the largest and smallest eigenvalues of  $A_{EE}$  can be bounded by*

$$\lambda_{\min}(A_{EE}) \geq \lambda_{\min}(A), \quad \lambda_{\max}(A_{EE}) \leq \lambda_{\max}(A).$$

*Proof of Lemma D.1.* By definition,

$$\lambda_{\min}(A_{EE}) = \inf_{\mathbf{x} \in \mathbb{R}^{|E|}} \frac{\mathbf{x}^T A_{EE} \mathbf{x}}{\mathbf{x}^T \mathbf{x}}.$$

Given  $\mathbf{x} \in \mathbb{R}^{|E|}$ , let  $\tilde{\mathbf{x}}$  denote its augmentation in  $\mathbb{R}^p$  such that the entries of  $\tilde{\mathbf{x}}$  indexed by  $E$  coincide with that of  $\mathbf{x}$ , and those indexed by  $E^c$  are equal to 0. Then

$$\lambda_{\min}(A_{EE}) = \inf_{\mathbf{x} \in \mathbb{R}^{|E|}} \frac{\tilde{\mathbf{x}}^T A \tilde{\mathbf{x}}}{\tilde{\mathbf{x}}^T \tilde{\mathbf{x}}} \geq \inf_{\tilde{\mathbf{x}} \in \mathbb{R}^p} \frac{\tilde{\mathbf{x}}^T A \tilde{\mathbf{x}}}{\tilde{\mathbf{x}}^T \tilde{\mathbf{x}}} = \lambda_{\min}(A).$$

The upper bound for  $\lambda_{\max}(A_{EE})$  is proved similarly.  $\square$

*Proof of Proposition 5.2.* Observe that

$$\|\Omega_{E^c E}(\Omega_{EE})^{-1}\|_\infty = \sup_{\mathbf{x} \in \mathbb{R}^{|E|}} \frac{\|\Omega_{E^c E}(\Omega_{EE})^{-1} \mathbf{x}\|_\infty}{\|\mathbf{x}\|_\infty}$$

$$\begin{aligned}
&= \sup_{\mathbf{y} \in \mathbb{R}^{|E|}} \frac{\|\Omega_{E^c E} \mathbf{y}\|_\infty}{\|\Omega_{EE} \mathbf{y}\|_\infty} \\
&= \sup_{\|\mathbf{y}\|_2=1} \frac{\|\Omega_{E^c E} \mathbf{y}\|_\infty}{\|\Omega_{EE} \mathbf{y}\|_\infty} \\
&\leq \frac{\sup_{\|\mathbf{y}\|_2=1} \|\Omega_{E^c E} \mathbf{y}\|_\infty}{\inf_{\|\mathbf{y}\|_2=1} \|\Omega_{EE} \mathbf{y}\|_\infty} \\
&\leq \sqrt{|E|} \cdot \frac{\sup_{\|\mathbf{y}\|_2=1} \|\Omega_{E^c E} \mathbf{y}\|_2}{\inf_{\|\mathbf{y}\|_2=1} \|\Omega_{EE} \mathbf{y}\|_2} \\
&\leq \left( |E| \cdot \frac{\sup_{\|\mathbf{y}\|_2=1} \mathbf{y}^T \Omega_{EE^c} \Omega_{E^c E} \mathbf{y}}{\inf_{\|\mathbf{y}\|_2=1} \mathbf{y}^T \Omega_{EE} \Omega_{EE} \mathbf{y}} \right)^{1/2} \\
&\leq \left( |E| \cdot \left( \frac{\sup_{\|\mathbf{y}\|_2=1} \mathbf{y}^T (\Omega_{EE^c} \Omega_{E^c E} + \Omega_{EE} \Omega_{EE}) \mathbf{y}}{\inf_{\|\mathbf{y}\|_2=1} \mathbf{y}^T \Omega_{EE} \Omega_{EE} \mathbf{y}} - 1 \right) \right)^{1/2} \\
&\leq \left( |E| \cdot \left( \frac{\lambda_{\max}((\Omega^2)_{EE})}{\lambda_{\min}((\Omega_{EE})^2)} - 1 \right) \right)^{1/2},
\end{aligned}$$

where we used the inequality that for any  $\mathbf{x} \in \mathbb{R}^p$ ,

$$\|\mathbf{x}\|_2 \leq \|\mathbf{x}\|_\infty \leq \sqrt{p} \|\mathbf{x}\|_2.$$

From Lemma D.1,

$$\lambda_{\max}((\Omega^2)_{EE}) \leq \lambda_{\max}(\Omega^2) = \lambda_{\max}^2(\Omega)$$

and

$$\lambda_{\min}((\Omega_{EE})^2) = \lambda_{\min}^2(\Omega_{EE}) \geq \lambda_{\min}^2(\Omega).$$

Hence the inequality can be further written as

$$\begin{aligned}
\|\Omega_{E^c E} (\Omega_{EE})^{-1}\|_\infty &\leq \left( |E| \cdot \left( \frac{\lambda_{\max}((\Omega^2)_{EE})}{\lambda_{\min}((\Omega_{EE})^2)} - 1 \right) \right)^{1/2} \\
&\leq \left( |E| \cdot \left( \frac{\lambda_{\max}^2(\Omega)}{\lambda_{\min}^2(\Omega)} - 1 \right) \right)^{1/2}.
\end{aligned}$$

It remains to derive the expressions for  $\lambda_{\min}^2(\Omega)$  and  $\lambda_{\max}^2(\Omega)$ . From Proposition 2.6,  $\Sigma$  has ordered eigenvalues

$$0 = \lambda_1 \leq \lambda_2 \leq \dots \leq \lambda_d,$$

with corresponding eigenvectors

$$\mathbf{u}_1 = \frac{1}{\sqrt{d}} \mathbf{1}, \mathbf{u}_2, \dots, \mathbf{u}_d.$$

Then  $\Sigma^* = \Sigma + M \cdot \mathbf{u}_1 \mathbf{u}_1^T$  is positive definite and has the same set of eigenvectors with corresponding eigenvalues

$$\tilde{\lambda}_1 = M, \lambda_2, \dots, \lambda_d.$$

Now consider the eigendecomposition of  $\Omega = \Sigma^* \otimes \Sigma^*$ . For any  $i, j$ , we have

$$\Sigma^* \mathbf{u}_i \mathbf{u}_j^T \Sigma^* = \lambda_i \lambda_j \cdot \mathbf{u}_i \mathbf{u}_j^T,$$



which implies that

$$\Omega \overline{\mathbf{u}_i \mathbf{u}_j^T} = \Sigma^* \otimes \Sigma^* \overline{\mathbf{u}_i \mathbf{u}_j^T} = \overline{\Sigma^* \mathbf{u}_i \mathbf{u}_j^T \Sigma^*} = \lambda_i \lambda_j \overline{\mathbf{u}_i \mathbf{u}_j^T}.$$

Hence each  $\overline{\mathbf{u}_i \mathbf{u}_j^T}$  is an eigenvector for  $\Omega$  with corresponding eigenvalue  $\lambda_i \lambda_j$ . It remains to show that  $\{\overline{\mathbf{u}_i \mathbf{u}_j^T}\}_{i,j}$  forms an orthonormal basis. For any  $(i, j), (i', j')$ ,

$$\overline{\mathbf{u}_i \mathbf{u}_j^T}^T \overline{\mathbf{u}_{i'} \mathbf{u}_{j'}^T} = \text{tr}(\mathbf{u}_i \mathbf{u}_j^T \mathbf{u}_{j'} \mathbf{u}_{i'}^T) = \begin{cases} 0, & j \neq j' \\ \text{tr}(\mathbf{u}_i \mathbf{u}_{i'}^T), & j = j' \end{cases} = \begin{cases} 0, & j \neq j' \\ 0, & j = j', i \neq i' \\ 1 & j = j', i = i' \end{cases}.$$

Therefore  $\Omega$  has the set of eigenvalues

$$\{\gamma_{ij}\}_{i,j} := \{\lambda_i \lambda_j\}_{i,j},$$

with eigenvectors

$$\{\mathbf{v}_{ij}\}_{i,j} := \{\overline{\mathbf{u}_i \mathbf{u}_j^T}\}_{i,j},$$

In particular, the smallest and the largest eigenvalues correspond to

$$\lambda_{\min}(\Omega) = \min_{i,j} \{\lambda_i \lambda_j\} = \min\{M^2, \lambda_2^2\}$$

and

$$\lambda_{\max}(\Omega) = \max_{i,j} \{\lambda_i \lambda_j\} = \max\{M^2, \lambda_d^2\}.$$

□

## E Block coordinate descent algorithm for the extreme graphical lasso

### E.1 Problem specification

In this appendix we present the algorithm for solving for  $\Theta$  given the input of  $S$  and  $c > 0$  from the following problem.

$$\min_{\Theta \succ 0} -\log |\Theta| + \text{tr}(S\Theta) + \lambda \sum_{i \neq j} |\theta_{ij} - c|. \quad (\text{E.1})$$

We slightly deviate from the notation from the rest of the paper. The  $\Theta$  here corresponds to the  $\Theta^*$  in the main text of the manuscript. This is to simply the notation in the following algebraic representations.

The classical graphical lasso requires  $c = 0$  instead of  $c > 0$ . Similar to  $c = 0$ , for  $c > 0$ , (E.1) is also a convex optimization. Therefore a unique solution exists and satisfies the KKT condition:

$$-\Theta^{-1} + S + \lambda \Gamma = \mathbf{0}, \quad (\text{E.2})$$

where  $\Gamma := \text{sign}(\Theta)$  is the sub-gradient of  $\sum_{i \neq j} |\theta_{ij} - c|$  satisfying

$$\gamma_{ij} = \begin{cases} \text{sign}(\theta_{ij} - c), & \theta_{ij} \neq c; \\ \in [-1, 1], & \theta_{ij} = c. \end{cases}$$

The algorithm presented in this appendix is adapted from the P-GLASSO algorithm proposed by Mazumder and Hastie (2012). While the most widely used algorithm for solving the classical graphical lasso is the GLASSO algorithm (Friedman et al., 2008), based on block coordinate descent, it cannot be directly adapted for the case of  $c > 0$ . The P-GLASSO algorithm is also based on block coordinate descent but solves for a different target function at each iteration. It has a similar order of computation as the GLASSO and is designed to avoid the computation incurred by inverting large matrices at each iteration.

## E.2 Block matrix inversion

In this algorithm we make use of the following result for the inversion of block matrices.

Let  $W$  be the inverse of  $\Theta$  such that  $W \cdot \Theta = I$ , where

$$\Theta = \begin{pmatrix} \Theta_{11} & \boldsymbol{\theta}_{12} \\ \boldsymbol{\theta}_{12}^T & \theta_{22} \end{pmatrix}.$$

Then

$$W = \begin{pmatrix} W_{11} & \mathbf{w}_{12} \\ \mathbf{w}_{12}^T & w_{22} \end{pmatrix} = \begin{pmatrix} (\Theta_{11} - \theta_{22}^{-1} \boldsymbol{\theta}_{12} \boldsymbol{\theta}_{12}^T)^{-1} & -\theta_{22}^{-1} W_{11} \boldsymbol{\theta}_{12} \\ \cdot & \theta_{22}^{-1} + \theta_{22}^{-2} \boldsymbol{\theta}_{12}^T W_{11} \boldsymbol{\theta}_{12} \end{pmatrix} \quad (\text{E.3})$$

$$= \begin{pmatrix} \Theta_{11}^{-1} + \frac{\Theta_{11}^{-1} \boldsymbol{\theta}_{12} \boldsymbol{\theta}_{12}^T \Theta_{11}^{-1}}{\theta_{22} - \boldsymbol{\theta}_{12}^T \Theta_{11}^{-1} \boldsymbol{\theta}_{12}} & -\frac{\Theta_{11}^{-1} \boldsymbol{\theta}_{12}}{\theta_{22} - \boldsymbol{\theta}_{12}^T \Theta_{11}^{-1} \boldsymbol{\theta}_{12}} \\ \cdot & \frac{1}{\theta_{22} - \boldsymbol{\theta}_{12}^T \Theta_{11}^{-1} \boldsymbol{\theta}_{12}} \end{pmatrix} \quad (\text{E.4})$$

where  $\cdot$  denotes the mirroring of elements in the upper triangle. The derivation can be found in Section E.5. The same formula can be applied for the opposite representation of  $\Theta$  using  $W$ .

## E.3 P-GLASSO algorithm

The algorithm operates by updating a specific row/column of  $\Theta$  ( $\Theta$  is symmetric) in each iteration while keeping the rest of the row/column fixed. The operation is repeated while iterating through the rows/columns until convergence. Write  $\Theta$  as

$$\Theta = \begin{pmatrix} \Theta_{11} & \boldsymbol{\theta}_{12} \\ \boldsymbol{\theta}_{12}^T & \theta_{22} \end{pmatrix}.$$

Consider the problem of estimating  $\boldsymbol{\theta}_{12}$  and  $\theta_{22}$  while keeping  $\Theta_{11}$  fixed.

Denote  $W$  as the inverse of  $\Theta$ . Then the KKT condition can be re-written as

$$-W + S + \lambda \Gamma = \mathbf{0}. \quad (\text{E.5})$$

First, (E.5) provides direct solutions to the diagonal entries of  $W$ :

$$w_{ii} = s_{ii} + \lambda \gamma_{ii} = s_{ii}.$$

The last column of (E.5) gives

$$-\mathbf{w}_{12} + \mathbf{s}_{12} + \lambda \gamma_{12} = \mathbf{0}. \quad (\text{E.6})$$

The lower left entry of the right hand side of (E.3) gives

$$\Theta_{11} \mathbf{w}_{12} + \boldsymbol{\theta}_{12} \cdot w_{22} = \mathbf{0},$$

which allows us to write  $\mathbf{w}_{12}$  as

$$\mathbf{w}_{12} = -\Theta_{11}^{-1} \boldsymbol{\theta}_{12} \cdot w_{22}.$$

Plugging into (E.6), we have

$$\Theta_{11}^{-1} \cdot \boldsymbol{\theta}_{12} w_{22} + \mathbf{s}_{12} + \lambda \cdot \text{sign}(\boldsymbol{\theta}_{12} - c\mathbf{1}) = \mathbf{0}.$$

Replacing  $w_{22}$  with the known solution  $w_{22}^* := s_{22} + \lambda$ , we have

$$\Theta_{11}^{-1} \cdot \boldsymbol{\theta}_{12} w_{22}^* + \mathbf{s}_{12} + \lambda \cdot \text{sign}(\boldsymbol{\theta}_{12} - c\mathbf{1}) = \mathbf{0}.$$

Here we reserve the notation  $w_{22}$  for the lower diagonal entry of the current  $W$  for reasons to be stated later. Denote

$$\boldsymbol{\alpha} := (\boldsymbol{\theta}_{12} - c\mathbf{1}) w_{22}^*.$$

Then

$$\Theta_{11}^{-1} \cdot \boldsymbol{\alpha} + \Theta_{11}^{-1} c\mathbf{1} \cdot w_{22}^* + \mathbf{s}_{12} + \lambda \cdot \text{sign}(\boldsymbol{\alpha}) = \mathbf{0}.$$

This equation is the KKT condition for the lasso problem

$$\min_{\boldsymbol{\alpha}} \left\{ \frac{1}{2} \boldsymbol{\alpha} \Theta_{11}^{-1} \boldsymbol{\alpha} + (\Theta_{11}^{-1} c\mathbf{1} \cdot w_{22}^* + \mathbf{s}_{12})^T \boldsymbol{\alpha} + \lambda \|\boldsymbol{\alpha}\|_1 \right\},$$

which can be solved using a standard lasso algorithm. Once  $\boldsymbol{\alpha}$  is solved,  $\boldsymbol{\theta}_{12}$  can be obtained from

$$\boldsymbol{\theta}_{12} = \frac{\boldsymbol{\alpha}}{w_{22}^*} + c\mathbf{1}.$$

Then  $\theta_{22}$  can be updated by

$$\theta_{22} = \frac{1}{w_{22}^*} + \boldsymbol{\theta}_{12}^T \Theta_{11}^{-1} \boldsymbol{\theta}_{12}, \quad (\text{E.7})$$

which follows from the matrix operation of inverses, see (E.4).

In principle, we can repeat the above procedure to iteratively update each row/column of  $\Theta$ . The estimated  $\Theta$  will guarantee to converge from the convergence of block gradient descent, see for example Proposition 2.7.1 of Bertsekas (1997). However, there is one extra consideration. We would like to avoid inverting large matrices, specifically in calculating  $\Theta_{11}^{-1}$ . Therefore we require an extra step for storing the updates in each iteration that proceeds as follows.

We propose to store all our updates from each iteration into the matrix  $W$  and pass it on to the next iteration:

- At the beginning of an iteration, given  $W$ , we can calculate  $\Theta_{11}^{-1}$  from

$$\Theta_{11}^{-1} = W_{11} - \mathbf{w}_{12}\mathbf{w}_{12}^T/w_{22}.$$

This follows from (E.4). Here  $w_{22}$ , the current lower diagonal entry of  $W$ , is used instead of  $w_{22}^*$ , in order to ensure the positive definiteness of  $\Theta_{11}^{-1}$ .

- At the end of an iteration, we can calculate the updated  $W$  from  $\Theta_{11}^{-1}$ ,  $\theta_{12}$  and  $\theta_{22}$  using the formula (E.4). The updated  $W$  is then carried on to the next iteration.

In both operations, only matrix multiplication is required, minimizing the computation incurred.

In the following we show that for each iteration, if the input  $W$  is positive definite, then the updated  $W$  will also be positive definite, hence ensuring that  $\Theta$  is positive definite throughout the iterations.

Assume that input  $W$  is positive definite. Then  $\Theta_{11}$ , which is fixed in the current iteration, is also positive definite. From the Schur complement lemma, the necessary and sufficient condition for the updated  $\Theta$  to be positive definite is

$$\theta_{22} - \theta_{12}^T \Theta_{11}^{-1} \theta_{12} > 0.$$

This is readily satisfied, as by the updating rule (E.7),

$$\theta_{22} - \theta_{12}^T \Theta_{11}^{-1} \theta_{12} = \frac{1}{w_{22}^*} > 0.$$

#### E.4 Pseudo code: P-GLASSO for extremes

- Input:  $S$ ,  $\lambda$  and  $c$ .
- Initiate  $W = S$ . (Or Initiate  $W = \text{diag}(S)$  and  $\Theta = W^{-1}$ .)
- Iterate until convergence. Input  $W$ . Output updated  $W$ .
  - Permute the rows/columns of  $W$  such that the target row/column is at the end of the matrix (i.e.  $\mathbf{w}_{12}$ ).
  - Compute  $\Theta_{11}^{-1}$  from input  $W$  via

$$\Theta_{11}^{-1} = W_{11} - \mathbf{w}_{12}\mathbf{w}_{12}^T/w_{22}.$$

- Let  $\boldsymbol{\alpha} := (\theta_{12} - c\mathbf{1})w_{22}^*$ , where  $w_{22}^* := s_{22}$ . Solve for  $\boldsymbol{\alpha}$  via

$$\boldsymbol{\alpha} = \arg \min_{\boldsymbol{\alpha}} \left\{ \frac{1}{2} \boldsymbol{\alpha}^T \Theta_{11}^{-1} \boldsymbol{\alpha} + (\mathbf{s}_{12} + cw_{22}^* \Theta_{11}^{-1} \mathbf{1})^T \boldsymbol{\alpha} + \lambda \|\boldsymbol{\alpha}\|_1 \right\}.$$

This solution can be written in a lasso regression form

$$\boldsymbol{\alpha} = \arg \min_{\boldsymbol{\alpha}} \left\{ \frac{1}{2} \|A\boldsymbol{\alpha} - \mathbf{b}\|_2^2 + \lambda \|\boldsymbol{\alpha}\|_1 \right\},$$

where  $A$  and  $\mathbf{b}$  satisfy

$$A^T A = \Theta_{11}^{-1},$$

(here  $\Theta_{11}^{-1}$  is positive definite and symmetric, hence  $A = A^T$  is symmetric as well,) and

$$A\mathbf{b} = -(\mathbf{s}_{12} + cw_{22}^* \Theta_{11}^{-1} \mathbf{1}).$$

Let the eigendecomposition of  $\Theta_{11}^{-1}$  be

$$\Theta_{11}^{-1} = Q\Lambda Q^T,$$

where the columns of  $Q$  consists of the eigenvectors of  $\Theta_{11}^{-1}$  and  $\Lambda$  is the diagonal matrix with whose diagonal values correspond to the eigenvalues of  $\Theta_{11}^{-1}$ . Then  $A$  and  $A^{-1}$  can be calculated from

$$A = Q\Lambda^{\frac{1}{2}}Q^T,$$

and

$$A^{-1} = Q\Lambda^{-\frac{1}{2}}Q^T.$$

– Update

$$\boldsymbol{\theta}_{12} = \frac{1}{w_{22}^*} \boldsymbol{\alpha} + c\mathbf{1}.$$

– Update

$$\theta_{22} = \frac{1}{w_{22}^*} + \boldsymbol{\theta}_{12}^T \Theta_{11}^{-1} \boldsymbol{\theta}_{12}.$$

– Update

$$\begin{aligned} W &= \begin{pmatrix} \Theta_{11}^{-1} + \frac{\Theta_{11}^{-1} \boldsymbol{\theta}_{12} \boldsymbol{\theta}_{12}^T \Theta_{11}^{-1}}{\theta_{22} - \boldsymbol{\theta}_{12}^T \Theta_{11}^{-1} \boldsymbol{\theta}_{12}} & -\frac{\Theta_{11}^{-1} \boldsymbol{\theta}_{12}}{\theta_{22} - \boldsymbol{\theta}_{12}^T \Theta_{11}^{-1} \boldsymbol{\theta}_{12}} \\ \cdot & \frac{1}{\theta_{22} - \boldsymbol{\theta}_{12}^T \Theta_{11}^{-1} \boldsymbol{\theta}_{12}} \end{pmatrix} \\ &= \begin{pmatrix} \Theta_{11}^{-1} + w_{22}^* \cdot \Theta_{11}^{-1} \boldsymbol{\theta}_{12} \boldsymbol{\theta}_{12}^T \Theta_{11}^{-1} & -w_{22}^* \cdot \Theta_{11}^{-1} \boldsymbol{\theta}_{12} \\ \cdot & w_{22}^* \end{pmatrix}. \end{aligned}$$

– Arrange the rows and columns of  $W$  back to the original order.

- Calculate the final estimate  $\Theta = W^{-1}$ .

## E.5 Proofs of (E.3) and (E.4)

We now prove the equations (E.3) and (E.4). From the block definition of  $W$  and  $\Theta$ ,

$$W_{11} \Theta_{11} + \mathbf{w}_{12} \boldsymbol{\theta}_{12}^T = I \tag{E.8}$$

$$W_{11} \boldsymbol{\theta}_{12} + \theta_{22} \cdot \mathbf{w}_{12} = \mathbf{0} \tag{E.9}$$

$$\mathbf{w}_{12}^T \Theta_{11} + w_{22} \cdot \boldsymbol{\theta}_{12}^T = \mathbf{0}^T \tag{E.10}$$

$$\mathbf{w}_{12}^T \boldsymbol{\theta}_{12} + w_{22} \cdot \theta_{22} = 1. \tag{E.11}$$

From (E.9),

$$\mathbf{w}_{12} = -\theta_{22}^{-1} W_{11} \boldsymbol{\theta}_{12}.$$

Plugging into (E.11),

$$w_{22} = \theta_{22}^{-1} (1 - \mathbf{w}_{12}^T \boldsymbol{\theta}_{12}) = \theta_{22}^{-1} + \theta_{22}^{-2} \boldsymbol{\theta}_{12}^T W_{11} \boldsymbol{\theta}_{12}.$$

From (E.8),

$$W_{11}^{-1} = \Theta_{11} + W_{11}^{-1} \mathbf{w}_{12} \boldsymbol{\theta}_{12}^T = \Theta_{11} - W_{11}^{-1} \theta_{22}^{-1} W_{11} \boldsymbol{\theta}_{12} \boldsymbol{\theta}_{12}^T = \Theta_{11} - \theta_{22}^{-1} \boldsymbol{\theta}_{12} \boldsymbol{\theta}_{12}^T$$

This proves (E.3).

Now we prove (E.4). From (E.8) and (E.10),

$$W_{11} = \Theta_{11}^{-1} - \mathbf{w}_{12} \boldsymbol{\theta}_{12}^T \Theta_{11}^{-1} \quad (\text{E.12})$$

$$\mathbf{w}_{12} = -w_{22} \Theta_{11}^{-1} \boldsymbol{\theta}_{12} \quad (\text{E.13})$$

Plugging (E.13) into (E.11),

$$w_{22} \theta_{22} - w_{22} \boldsymbol{\theta}_{12}^T \Theta_{11}^{-1} \boldsymbol{\theta}_{12} = 1$$

and consequently,

$$w_{22} = \frac{1}{\theta_{22} - \boldsymbol{\theta}_{12}^T \Theta_{11}^{-1} \boldsymbol{\theta}_{12}}. \quad (\text{E.14})$$

Plugging (E.14) into (E.13),

$$\mathbf{w}_{12} = -\frac{\Theta_{11}^{-1} \boldsymbol{\theta}_{12}}{\theta_{22} - \boldsymbol{\theta}_{12}^T \Theta_{11}^{-1} \boldsymbol{\theta}_{12}}.$$

Plugging (E.14) into (E.12),

$$W_{11} = \Theta_{11}^{-1} + \frac{\Theta_{11}^{-1} \boldsymbol{\theta}_{12} \boldsymbol{\theta}_{12}^T \Theta_{11}^{-1}}{\theta_{22} - \boldsymbol{\theta}_{12}^T \Theta_{11}^{-1} \boldsymbol{\theta}_{12}}.$$

This proves (E.4).